1983

Investigation of resolution loss in contact exposure of transparent electrophotographic films

Thomas Charles Sutter

Investigation of Resolution Loss in Contact Exposure of Transparent Electrophotographic Films

by

Thomas Charles Sutter

A thesis submitted in partial fulfillment
of the requirements for the degree of
Master of Science in the School of
Photographic Arts and Sciences in the
College of Graphic Arts and Photography
of the Rochester Institute of Technology

December, 1983

Signature of the Author Thomas C. Sutter
Imaging and Photographic Science Division

Accepted by Ronald Francis
Coordinator, M.S. Degree Program

College of Graphic Arts and Photography
Rochester Institute of Technology
Rochester, New York

CERTIFICATE OF APPROVAL

M.S. DEGREE THESIS

The M.S. Degree Thesis of Thomas Charles Sutter
has been examined and approved
by the thesis committee as satisfactory
for the thesis requirement for the
Master of Science degree

Ronald P. Lubianez

Dr. Ronald Lubianez, Thesis Advisor

Willem Brouwer

Dr. Willem Brouwer

Vito DePalma

Dr. Vito DePalma

1/31/84

Date

THESIS RELEASE PERMISSION FORM

ROCHESTER INSTITUTE OF TECHNOLOGY
COLLEGE OF GRAPHIC ARTS AND PHOTOGRAPHY

Title of Thesis Investigation of Resolution Loss in Contact Exposure of Transparent Electrophotographic Films

I, Thomas C. Sutter, hereby (grant, ~~deny~~) permission to the Wallace Memorial Library of R.I.T. to reproduce my thesis in whole or in part. Any reproduction will not be for commercial use or profit.

Date 1/31/84

Investigation of Resolution Loss

in Contact Exposure of

Transparent Electrophotographic Films

by

Thomas Charles Sutter

Submitted to the
Imaging and Photographic Science Division
in partial fulfillment of the requirements
for the Master of Science Degree
at the Rochester Institute of Technology

Abstract

A study was performed to determine the nature of the effects causing resolution loss in contact exposure Transparent Electrophotographic (TEP) films. Target and TEP film characteristics were varied and resolution was measured under magnification. Results indicated that the factors responsible for resolution loss included the grain structure of the original target, moisture content of the target emulsion, and surface charge of the target. No conclusions could be made for the effect of TEP photoconductor coating thickness.

ACKNOWLEDGEMENTS

In appreciation of their support and assistance in completing this thesis, I would like to recognize the following individuals:

Dr. Ronald Lubianez of James River Graphics, Inc., South Hadley, M A., for his time and support as thesis advisor;

Dr. Vito DePalma of Castle Division of Sybron, Rochester, N.Y.;

Dr. Willem Brouwer of the R.I.T. Imaging and Photographic Science Division; and,

Dr. Thomas Fredericks of the R.I.T. Biology Department for his Scanning Electron Microscope work.

The support of James River Graphics, Inc. in supplying the materials and information for this work is also greatly appreciated, as is the support of the Central Intelligence Agency.

TABLE OF CONTENTS

LIST OF TABLES

LIST OF FIGURES

I. Introduction

The interest at Scott Graphics, Inc. in Transparent Electrophotographic (TEP®) film originated when the System 200 microfiche equipment was first introduced by Scott Graphics, Inc. as a convenient, high capacity storage medium with the extra advantage of add-on capability.[1] The USAF later began testing the film as a possible Laser Beam Recording (LBR) medium and as an aerial duplicating film.[1] Inherent properties of the system made it attractive for both purposes:[2]

1) sensitivity over almost the entire visible spectrum depending on the sensitizing dye used;
2) low RMS granularity and Wiener spectrum (directly related to the electrodeveloper quality);
3) high storage capacity (at low densities);
4) long shelf life (the charging acts as a gating mechanism);
5) dimensional stability;
6) archival permanance (the images are composed of carbon particles fused in an inert polymer matrix);
7) add-on capability;
8) positive or negative imaging with the same film;
9) D-max as high as 4.0;
10) variable contrast from 0.8 to 4.0.

A) Film Structure

The imaging process for TEP film is diagrammed in Figure 1. The three layer design consists of a polyester substrate, a transparent

metallic conductive layer which acts as a grounding plane during charging and processing, and an organic photoconductor layer consisting of a phenylene-diamine derivative homogeneously dispersed in a dielectric polymeric binder.[3] Characteristics of the particular film used in this research are listed in Appendix A.

B) Process

The film has an inherent amount of photoconductivity due to dissociation of the organic photoconductor (OPC) through phototropism.[3] When charged electrostatically, however, an amplification of 100,000 is obtainable (amplification in this case is defined as the number of carbon atoms deposited for each photon absorbed).[2] An image is formed by a signal dependent discharge proportional to the level of illumination. This allows for continuous tone recording. The actual latent image is formed by the photogeneration of a pair of charged carriers which migrate to opposite surfaces of the film under the influence of an internal electric field. These charge carriers then become trapped at the surface by neutralizing the electrostatic surface charge.

The complete process for imaging on TEP film is shown in Figure 2. The procedure is characteristic of most charged pigment xerographic systems: corona charging, exposure, toner development, and fixing. The developer used in this system is a liquid electrodeveloper composed of charged carbon particles suspended in a dielectric liquid.[4] The charge on the toner particles arises from their electrokinetic relationship with the surrounding liquid.[5] The development depends on the electrophoretic migration of the particles through solution under the influence of the electric field exerted by the image patterns.[6]

Fixing of the deposited toner is accomplished by fusing of the OPC

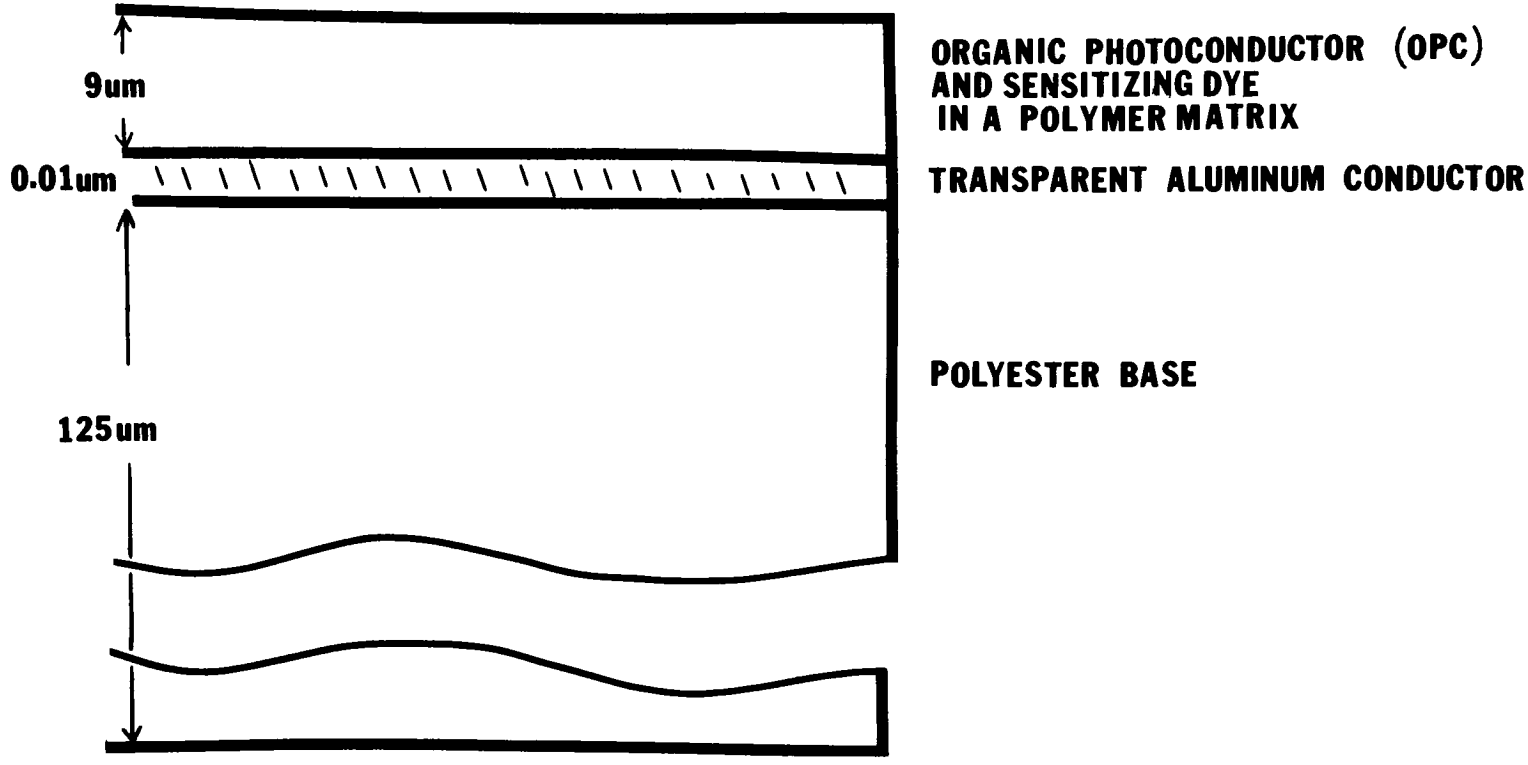

Figure 1. Construction of TEP film (type P5-003).

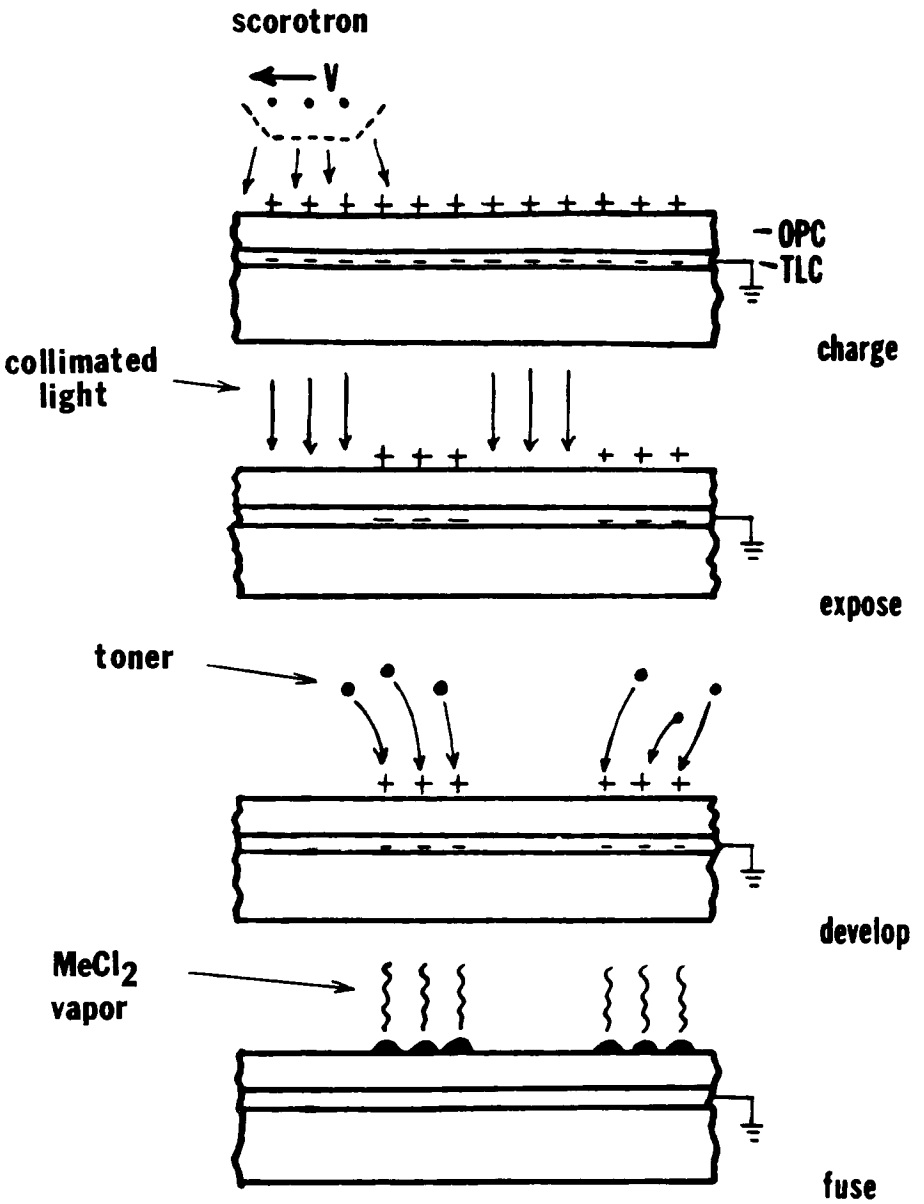

Development is by immersion in liquid electrodeveloper.
Fusing is by methylene chloride vapor used to soften binder.
Positive charging is shown.

Figure 2. Image formation in the TEP system.

C) Resolution

One of the most attractive aspects of the system is its resolving power capacity. Theoretically, the limit of resolution is determined by the finite size of the toner particles or clusters of particles used to make the image visible. Experimental developers have been formulated which greatly reduce the particle size effect and give resolution ranges equalling some of the best silver halide materials.[7]

Resolutions of almost 800 lp/mm have been obtained repeatably with micro-camera exposures of low contrast (6.6:1) targets on a film processed to an average gradient of 1.0 with an experimental negative working developer.[8] Using the James River Graphics P4-008 film with T48-5K developer, Perkin Elmer micro-camera results gave a peak resolution of 362 lp/mm.[8] Contact exposure work done by James River Graphics gave results of about half the micro-camera results, 100 to 150 lp/mm depending on test conditions used.[10] A variety of factors can affect the resolution: the choice of film/developer combination, polarity of charging, contrast of original and final images, exposure level, and to a degree, ambient conditions.

The most interesting effect, however, is the difference in resolution when a target is contact exposed as compared to a micro-camera exposure under identical conditions (i.e. charging, processing, etc.). When conditions are maintained constant, except for exposing method, the resolution obtained after contact exposure is usually half that of the micro-camera exposure.[9] The mechanism of this loss is not understood, but attempts at correcting the problem have been made. The effect would have to be occuring during the actual exposing step since the pre- and post-exposure handling of the film is the same for both trials.

A test was run at James River Graphics to determine the effect of a matte particle coating on the original targets. The conclusions were that no observable change in resolution resulted, probably due to the extremely thin layer used.[9] A second test was made to see if moisture retained in the gelatin of the original target was responsible for altering the electric fields of the image due to conductivity. The results showed that resolution actually decreased with reduced moisture content; however, the extent of the test was limited to only two moisture levels.[9] In a third test the original target was overcoated with a 0.25 micron non-conductive acrylic layer. Once again there was a loss in resolution. No explanation was offered.[9]

The most promising test was based on the premise that a charge transfer between sheets was responsible for the resolution loss.[11] The target in this case was charged to an identical apparent surface voltage (ASV) as the TEP film prior to contacting. Losses in resolution were reduced but not completely returned to micro-camera levels.

A final test was performed to determine the effect of the thickness of the OPC layer on resolution.[12] Once again the limited range of the experiment resulted in no observable change.

One additional hypothesis, which remains untested, is that of optical scattering from the original target emulsion.[13] In a projection exposure system the light rays passing through the target are focused by a lens system and arrive at the surface of the OPC at normal incidence, resulting in a minimum spreading and off-axis exposure. In a contact situation, the amount of scattering by the silver grains is large and the relatively thick OPC layer allows for a great deal of off-axis exposure,

(see Figure 3). The result, therefore, would be an overall lowering of resolution due to unwanted exposure.

D) Present Work

The hypothesis presented here is that the resolution loss is not attributable to an optical effect or an electrical effect acting alone, but rather to contributions from both.

The optical scattering phenomenon is a complex problem, compounded by the structure of the TEP film. The background density of the film ranges from 0.05 for the ionic conductors and semi-conductors to 0.40 for the metallic types.[14] The low density is a necessity of the film design, but it is also an indication of the low absorption of the OPC layer. Dirks[15] reports that this property minimizes scatter in the layer during exposure and hence improves resolution. This would be reasonable for a projection system where the rays arrive normal to the surface and have little or no refraction to cause off-axis exposures, but the contact exposure case is complicated by this property.

The target of greatest interest is the low contrast one, typical of the type of aerial imagery which would be duplicated. The low density allows a great deal of light to pass through the emulsion and to be scattered by the random grain structure. The scattering of the light can be characterized by the Callier Q factor which relates the specular (narrow angle transmission) density to the diffuse density of an emulsion by

$$Q = \text{specular D} \; / \; \text{diffuse D} \quad .$$

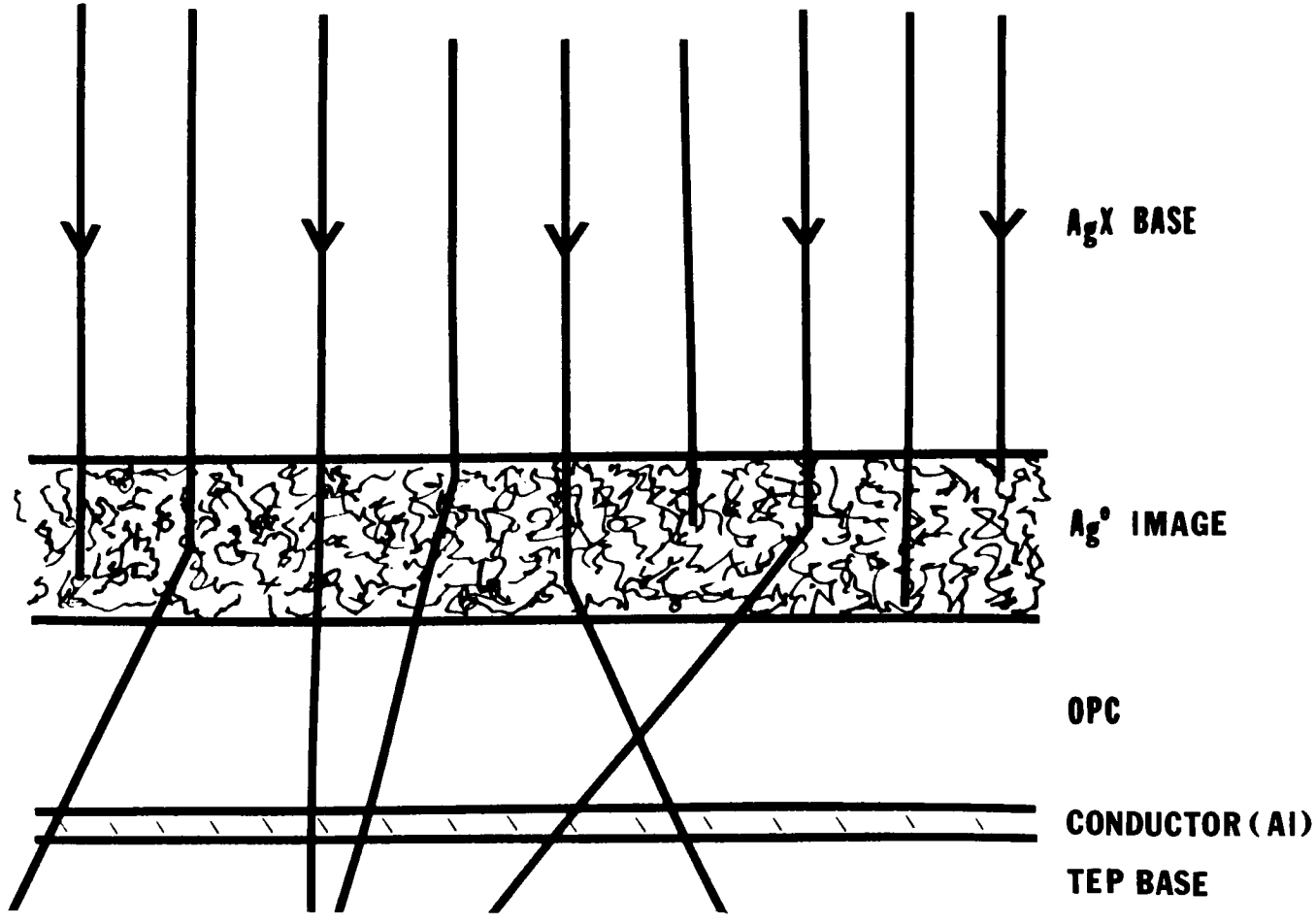

Figure 3. Scattering of light rays by silver halide emulsion during contact exposure of TEP film.

The image forming light is then allowed to enter the OPC layer without any optical correction. These oblique angles of entry cause latent image formation in non-image areas due to optical spread. Since the photo-active molecules are homogeneously in solution throughout the 9 micron thick layer, the off-axis rays may travel a great distance laterally before finally being absorbed. This would reduce the resulting surface resolution after charge carrier migration.

Until now, internal reflections have been neglected. The above system assumes perfect contact and no additional reflections or refractions.

The indexes of refraction (n) for gelatin and the acrylic/vinyl TEP binder are both in the range of 1.50-1.55 for the wavelengths of interest.[16,17] Snell's law predicts the degree of deviation from the normal at a boundry as function of incident angle Θ_1 and the indexes of refraction of the two materials;

$$n_1 \sin \Theta_1 = n_2 \sin \Theta_2$$

or $$\sin \Theta_2 = (n_1/n_2) \sin \Theta_1.$$

If the gelatin and OPC layers are in perfect contact, the degree of deviation is very small since the difference in the indexes of refraction across the boundry is close to zero;

$$\sin \Theta_2 = \sin \Theta_1.$$

The case of perfect contact is idealistic since a thin layer of air will almost always remain due to the microscopic defects in the surface and contaminants such as moisture and dust. This air layer has the effect of adding one more interface and increasing the deviation of the ray because of the change in index of refraction. (An index of n = 1.0 is assumed for air.) For the boundary between the gelatin and the air,

$$\sin \Theta_2 = 1.5 \sin \Theta_1$$

and for the air layer/OPC layer boundary,

$$\sin \Theta_3 = 0.67 \sin \Theta_2.$$

Figure 4 shows that the lateral displacement of the final photon absorption site from the site of initial incidence is a function of the initial deflection angle, Θ_1, the initial depth of the deflection site within the emulsion, X_1, the air gap thickness, X_2, and the depth of the absorption site in the OPC layer, X_3.

The total lateral displacement is given by

$$L = L_1 + L_2 + L_3$$

where, $L_1 = X_1 \tan \Theta_1$

$L_2 = X_2 \tan \Theta_2$

and $L_3 = X_3 \tan \Theta_3$.

Applying Snell's law,

$$L_1 = X_1 \tan \theta_1$$

$$L_2 = X_2 [\tan(\arcsin(1.5 \sin \theta_1))]$$

and $$L_3 = X_3 \tan \theta_1.$$

In order to simplify these equations we can make the approximation of $\sin \theta \cong \theta$ when θ is in radians. For angles less that 20 degrees (0.35 radians) the error is only 2 percent. This approximation can be extended to allow arc sin $(1.5 \sin \theta) \cong 1.5\theta$ with an error of only 3 percent for angles of less than 0.35 radians.

The above equation can then be simplified to

$$L = (X_1 + X_3) \tan \theta_1 + X_2 \tan (1.5\ \theta_1).$$

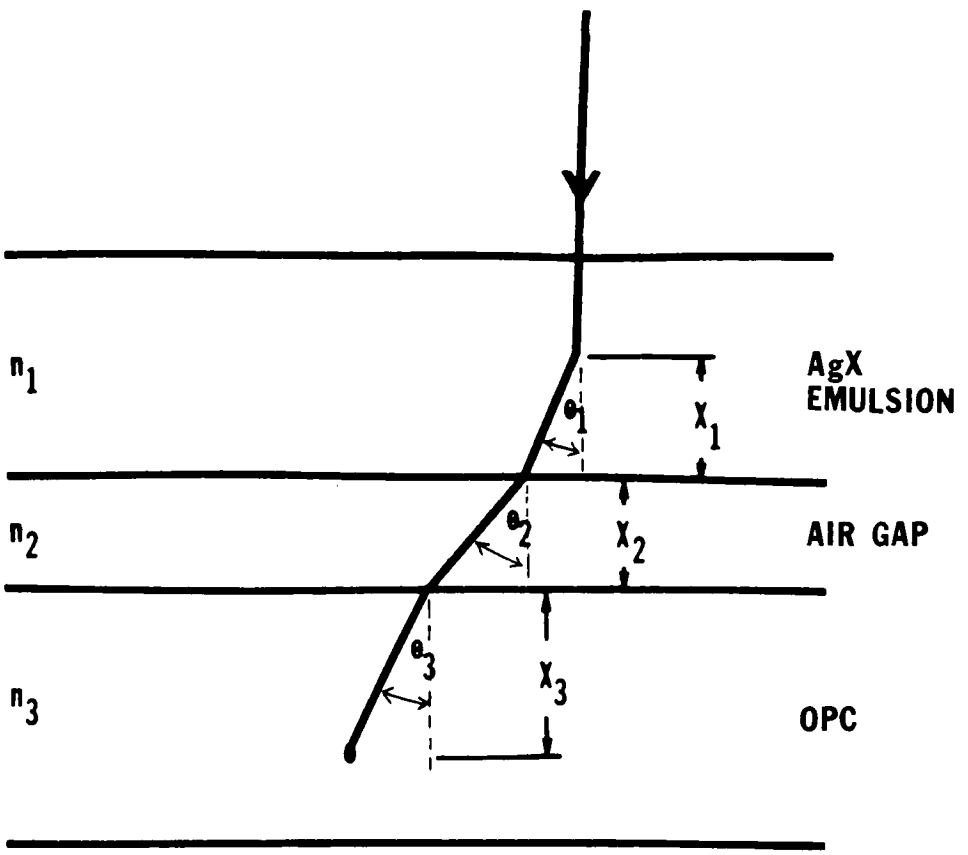

n_1 = index of refraction of gelatin
n_2 = index of refraction of air (=1.00)
n_3 = index of refraction of OPC polymer binder
θ_1 = initial angle of deflection
θ_2 = first refracted angle
θ_3 = second refracted angle
X_1, X_2, X_3 = depth in each layer

Figure 4. Lateral displacement of image point resulting from deflection in silver halide emulsion.

Figure 5 gives the lateral displacement as a function of air gap for several angles of deflection. In this case the data is computed using an average distance for X_1 and X_3 (the depth of deflection in the silver emulsion and TEP OPC layer respectively), and assumes only a single deflection takes place. In the actual case, a single photon may be affected several times in its course through the emulsion.

The result of the deflection shown in Figure 4 is to cause spreading of the final image, thus lowering resolution. Even if the air gap, X_2, is reduced to zero, as in an ideal contact situation, the final surface displacement of an image point would be over 2.5 um for angles of about 16 degrees or greater. (See Figure 5.)

As an example, if enough exposure is caused at an average lateral displacement of 2.5 um, the final image resolution would be limited to 200 lp/mm. This results because the distance of displacement is equivalent to the width of one line at this frequency. (See Appendix J.)

The optical effect has one further complication which can lower resolution; multiple internal reflections. At an interface of two layers where a change in index of refraction is encountered, a certain amount of the incident ray penetrates the second layer, but a portion of the light is reflected back into the original medium.[18] This reflection phenomenon can continue until the intensity of the light is diminished to levels which cannot affect exposure. Until this level is reached, however, unwanted image exposure can be produced causing lateral spread of the original image. The amount of the spread is dependent on the intensity of the light (governing how many of the reflections will produce images), the indexes of the layers, the thickness of each layer, and the incident

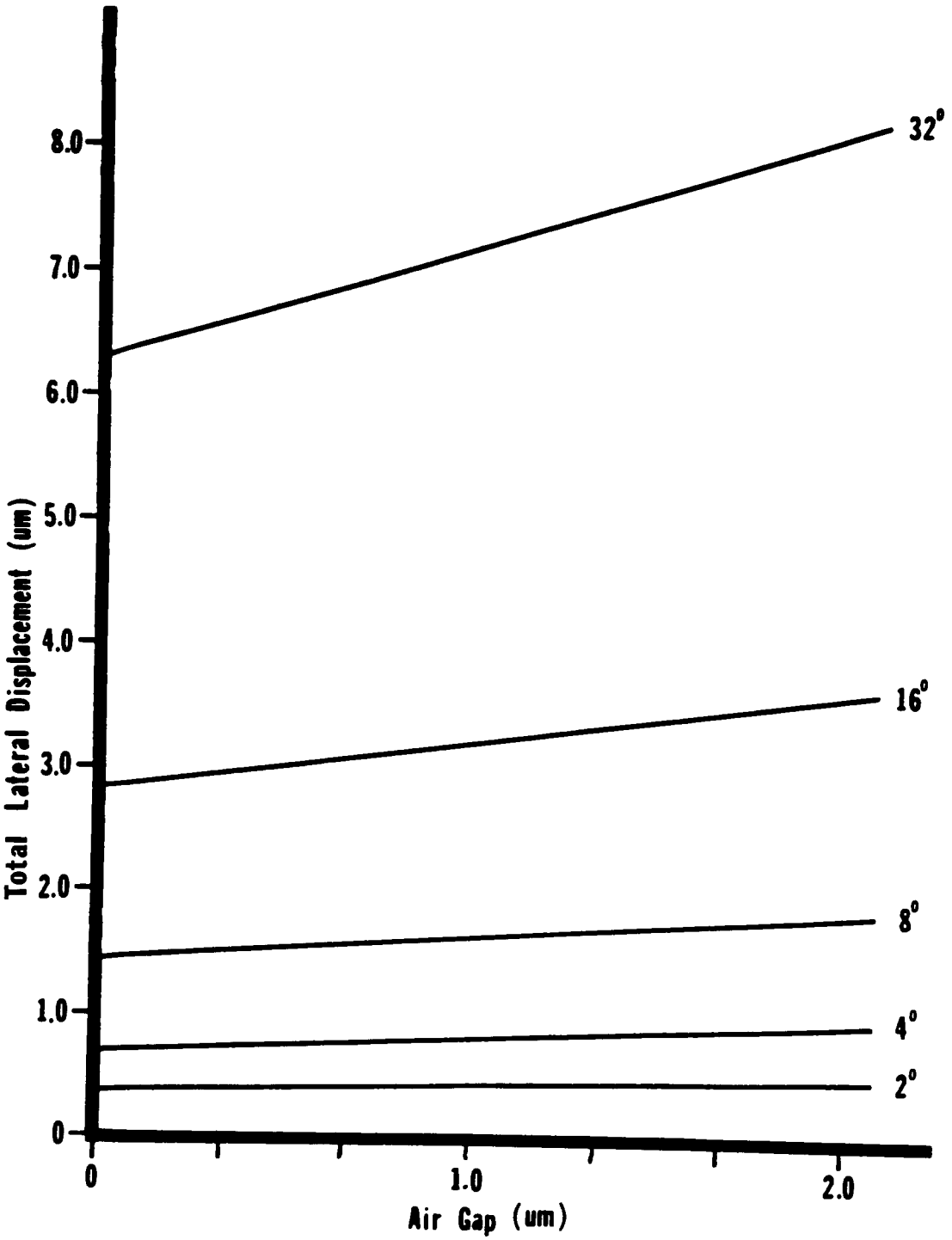

Figure 5. Total resulting image displacement as a function of air gap and initial angle of deflection.

angle. It can be seen in Figure 6 that a ray which is nearly normal to the surface has a restricted range of reflection. In this case the reflections can actually aid density build-up by increasing the chances for photon absorption. This technique is used in Reflex Xerography where the internal reflections are enhanced by a mirrored substrate to increase density.[19]

As the angle of incidence is increased, the amount of displacement and the amplitude of the reflection increases, causing greater image spreading. The low density of the OPC layer allows for a greater travel distance from the point of entry before absorption.

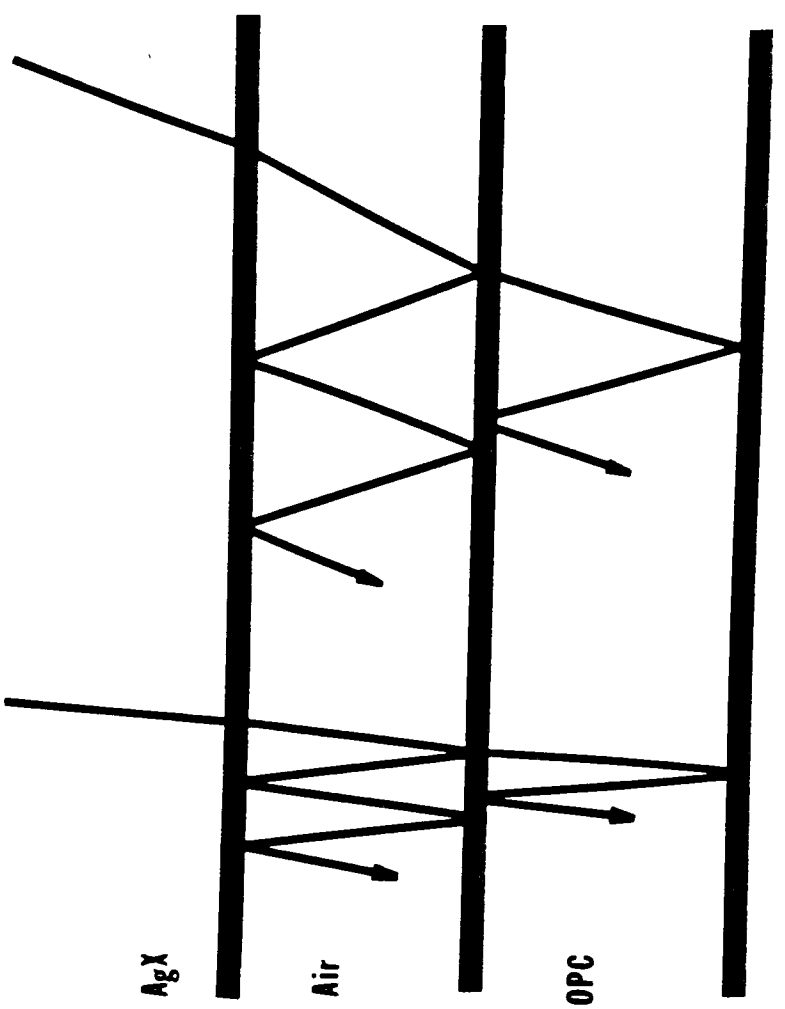

Figure 6. Internal reflections resulting from initial deflection of light ray in silver halide emulsion. Lateral displacement of image point depends on angle of deflection. (Not to scale).

The portion of unpolarized light reflected from the surface of a dielectric is given by [20],

$$R = 0.5[(\sin^2(\Theta-\Theta')/\sin^2(\theta+\theta') + (\tan^2(\theta-\theta')/(\tan^2(\theta+\theta')]$$

where Θ and Θ' are the incident and refracted angles respectively. At normal incidence the equation reduces to

$$R = (n'-n)^2/(n'+n)^2.$$

If I is the incident ray intensity, then each successive transmitted and reflected ray can be denoted by the product of the transmission, (t), or reflection, (r), at each interface and the intensity. Each successive intensity will be a fraction of the previous since the transmittance, (t), or reflection, (r), is always less than one. Figure 7 shows the reflection of an incident ray and Table 1 predicts the intensity of the ray at each point.

As can be seen from Table 1, the first reflected ray in the air gap is just 4% of the incident intensity, and after being re-reflected off the gelatin, the amount of light left to penetrate the OPC layer is only 0.15% (a reduction of about 9.5 stops). The probabilty of forming an image with this intensity is low, but if exposure did happen, the surface displacement of the image for a 1.0 micron air gap and 30 degree angle would only be about 1.7 microns. (See Figure 7.)

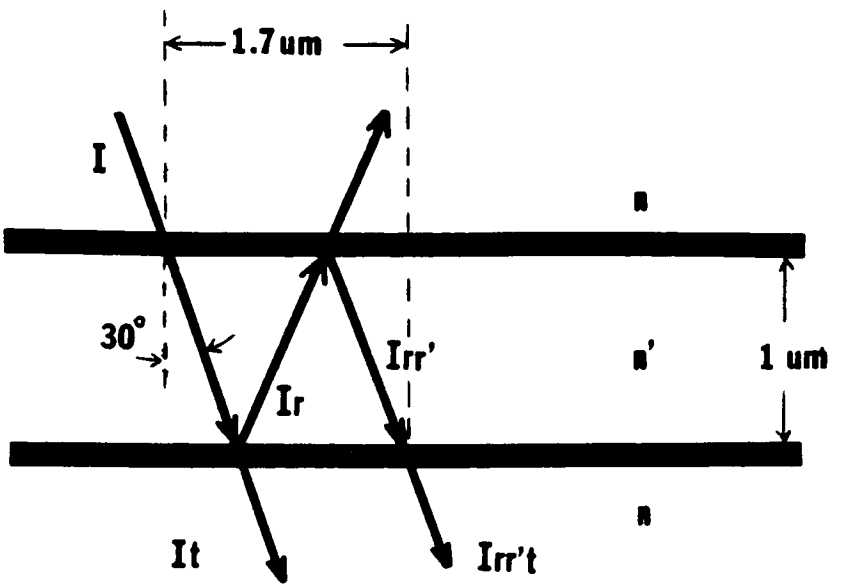

I = intensity of image forming ray as it leaves the target.
r = reflectivity of OPC surface.
t = transmittance of OPC surface.
r'= reflectivity of target surface.
n = index of refraction of gelatin and OPC polymer binder.
n'= index of refraction of air

Figure 7. Reflection and transmission of ray during contact exposure. A 1 um air gap is present.

θ	Intensity of Ray*			
	It	Ir	Irr'	Irr't
0	0.960	0.040	1.60E-3	1.54E-3
5	0.960	0.040	1.60E-3	1.54E-3
10	0.960	0.040	1.60E-3	1.54E-3
15	0.960	0.040	1.61E-3	1.54E-3
20	0.960	0.040	1.62E-3	1.56E-3
25	0.959	0.041	1.65E-3	1.59E-3
30	0.958	0.042	1.72E-3	1.65E-3
35	0.957	0.043	1.85E-3	1.77E-3

*I = 1.000

Table 1. Intensity of ray after encountering interfaces between films.

Another problem is the possibility of internal reflections within the OPC layer because of its thickness (9 microns). That same ray incident on the surface at 30 degrees will be laterally displaced by 6.4 microns upon reaching the OPC/air interface after being reflected from the conducting layer. (see Figure 8.) The actual photon absorption could take place anywhere along this path.

Since the reflectivity of the semi-transparent aluminum layer is not known at this time, the actual intensity of this reflected ray cannot be predicted.

If the refraction and reflection effects are combined the result can give an even worse case of image spread. If a ray starts with a 30 degree deflection in the silver halide emulsion at a depth of 5 um, passes through a 1 um air gap, and reflects off the conductive layer of the TEP before being absorbed near the surface of the OPC, (see Figure 9), the final lateral displacement of the image point would be 14 um.

This could affect resolution below 100 lp/mm. This is an extreme case, but is used as an example of how these mechanisms can affect the final image resolution.

A problem of a different nature is evident when the electrostatic behavior of the film is examined. Before investigating the problem, the mechanism of image formation must be described.

The first step in the process involves charging the dielectric film to a predetermined surface voltage through corona discharge in air. Passing 6 to 8 kilovolts through a partially shielded thin wire causes ionization of the surrounding gases, generating charge carriers. In a positive corona the carrier species is hydrated protons, $(H_2O)_nH^+$, with n = 1, 2, 3....etc., depending on the RH, and in the

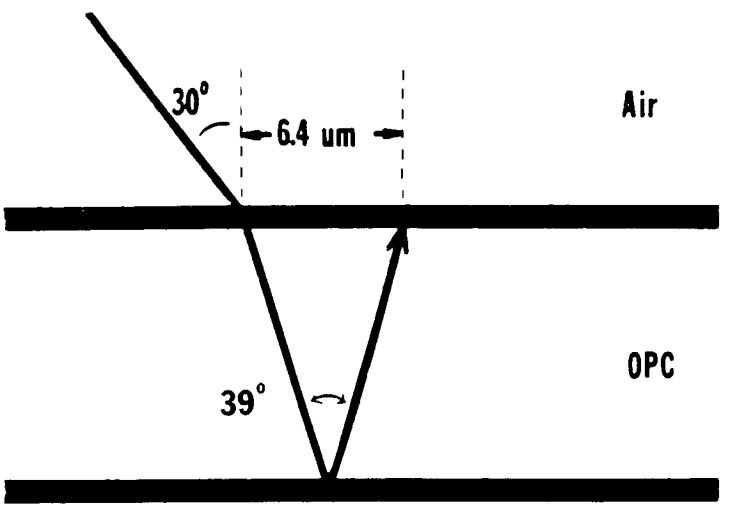

Ray is shown to reflect off the lower OPC surface and is absorbed at the upper surface.

Figure 8. Resulting image point displacement of a ray incident on the OPC surface at 30°.

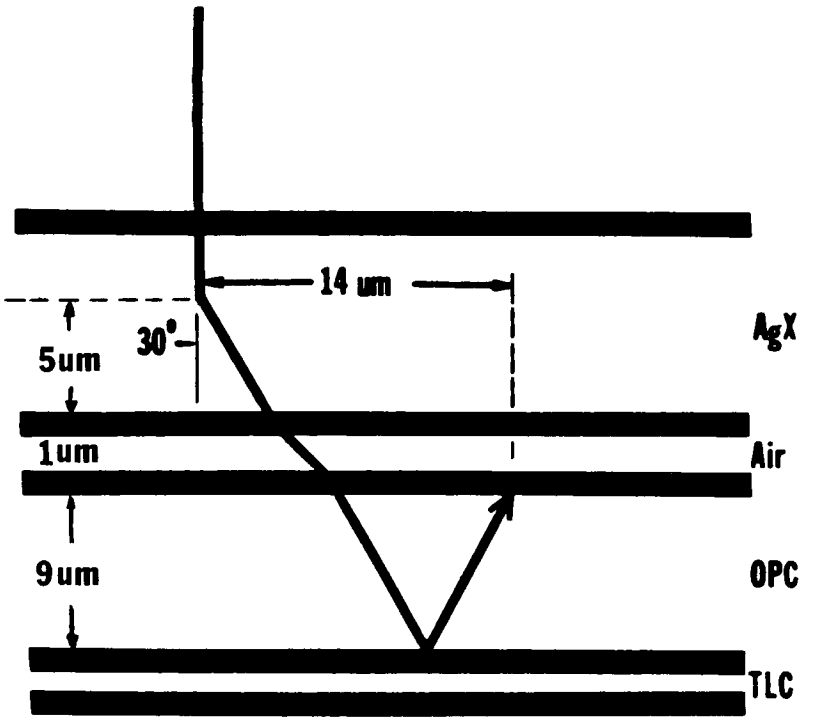

Figure 9. Resulting image point displacement due to a combined effect of deflection in the target, refraction at the interfaces, and reflection at the lower OPC boundary. Initial deflection is 30° at a depth of 5 um in the emulsion.

negative corona the species is predominately CO^-_3 and the hydrated forms $CO^-_3(H_2O)_{1,2}$.[25] These carriers then travel through free space and deposit a charge on the surface of the film. Grounding the conductive layer of the film serves to supply charges of opposite polarity for the other surface of the dielectric. The free surface of the OPC may act as a blocking layer, preventing the injection of charges into the bulk.[22] The actual mechanism of charge attachment is not completely understood but may be attributed to either the electrical attraction of charges of opposite polarity or some form of subsurface trap state.[23]

As charging progresses, the flow of charges from the ground layer to deep traps continues. As these traps become filled, a static space charge builds, opposing a further flow of charges. When the corona current is removed, a dark current is still evident due to an emptying of traps from the overfilled space charge field.[24]

The image forming mechanism during exposure involves the photogeneration of a pair of mobile charge carriers and the displacement of each to their corresponding surfaces.[25] The migration of the carriers is not a simple drift movement, but rather, a complex series of interactions with trapping states.[26]

Figure 10 is a cross-sectional view of the OPC layer.[27] Distance is shown vertically and electron energy is shown horizontally. Electron and hole traps are shown as vertical lines within the central OPC section.

After generation, the charge carriers move through transport states while influenced by the presence of the internal electric field. The transport states are made up of series of "fast" traps, traps with a very short release time. Slower traps, separated by electrophotographic

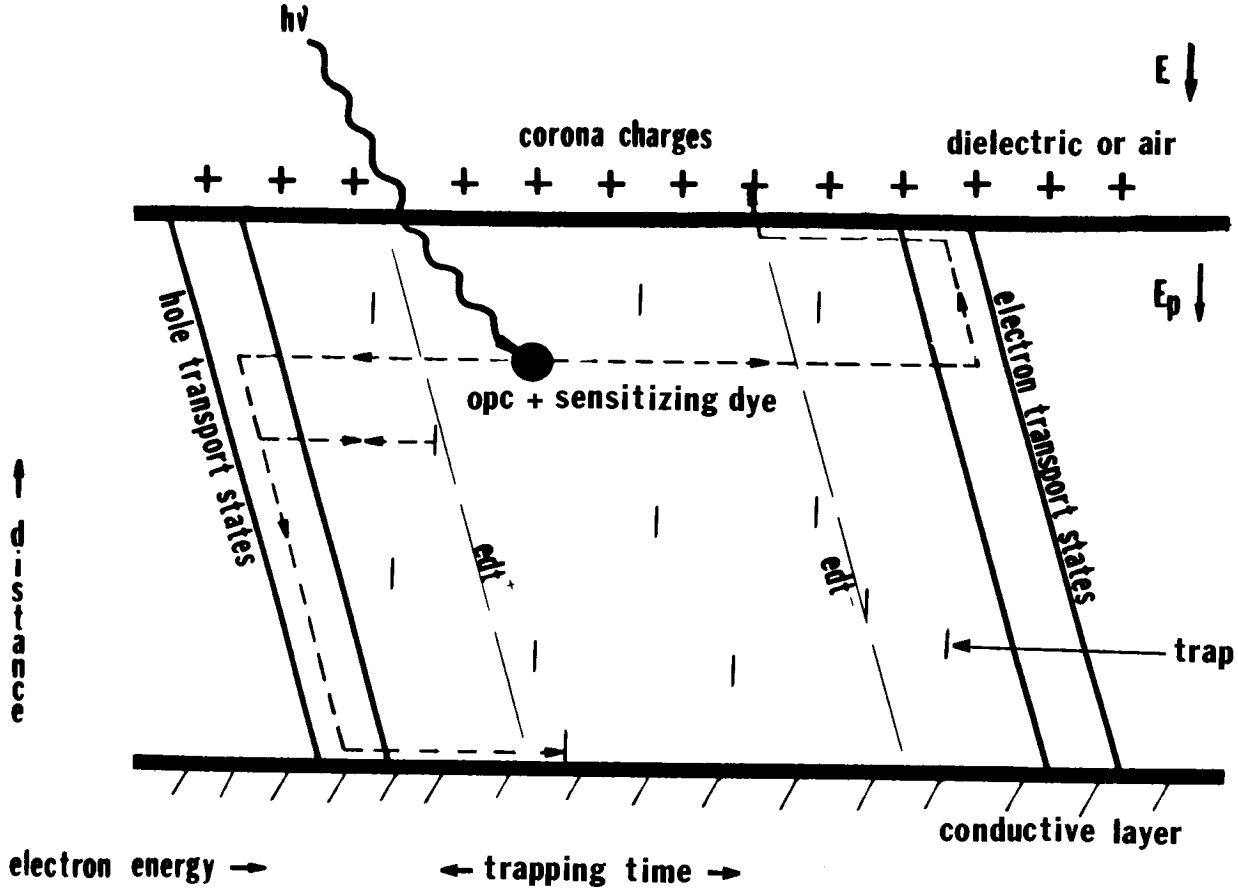

Electron energy increases to the right, distance is shown vertically, and trapping time increases horizontally outward from the center of the diagram.

Figure 10. Energy diagram of image formation in a photoconductor layer.

demarcation times, have longer release times, longer than the time required for processing. The electrophotographic demarcation times, (edt^+ and edt^-), are plotted with time of release increasing horizontally outward from the center of the diagram. The positions are relative and depend on the OPC matrix material. Movement from trap to trap is probably due to a "hopping" mobility characterized by a release time and a simultaneous spatial displacement due to the disordered nature of the layer.[28] The binder material used may also affect this trapping mechanism.[29]

The following description and equations are hypothesized by Mort and Pai.[26] The situation presented has similarities to the conditions of the material used in this study. Although these equations may not relate to the James River Graphics TEP film exactly, (the mechanism is not completely understood), they are postulated to give a representation of a lateral conduction mechanism which may be responsible for some resolution loss.

The fate of the carrier is primarily a function of the binder layer characteristics. The traps which act as transport states necessarily have release times, T_r, that are much less than the total transport times, T_t. This allows for a motion which simulates a free translational mobility.[28] If the carrier encounters a "slow" trap, one with a release time much greater than T_t, that part of the image dipole may never reach the surface. If the release time for the slow trap is greater than the time for processing, that carrier effectively becomes "fixed" for that part of the image.[26]

Hence, for an image to be generated at the surface, the carrier must overcome several time restrictions.[26]

If T_i, and T_{ri} are designated as the capture time from, and release time to the transport states for the i^{th} kind of trap, then the mean

transit time, T_t, for the carrier is given by

$$T_t = T_o + \Sigma_i \ (N_i T_{ri})$$

where $T_o = L/uE_p$ is the transit time for a carrier not trapped at all, $N_i = L/uT_iE_p$ is the expected number of times a carrier is trapped in the ith kind of trap, L is the thickness of the OPC layer, u is the carrier mobility, and E_p is the electric field inside the OPC layer.

Substituting,

$$T_t = (L/uE)[\ 1 + \Sigma_i(T_{ri}/T_i)]$$
$$= L/BuE$$

where $B = (\ 1 + \Sigma_i(T_{ri}/T_i)\ )^{-1}$, and E is the external field of the contacting dielectric or air next to the OPC layer.

Therefore, the total transit time, T_t, must be less than the processing time, T_p,

$$T_t = L/BuE < T_p$$

or the image will not effect a permanent, developable change. (Note that for development where a bias electrode is used, E may be different from the field during exposure and this may also affect movement of the carriers during processing.)

Also, the carrier lifetime, T_L, must be greater than the transit time,

$$T_L/B > T_t \ .$$

If these conditions are met, the carrier should ultimately reach the surface where the corona charges are located. These charges effectively

carriers.[26] The fate of the carrier, however, is still not completely characterized.

If sufficient recombination centers are present on the surface, trapping will occur rapidly, (T_s, the surface trapping time, is short), and latent images will form. For longer intervals the carrier fate remains undecided for a time $t < T_s$. If another dielectric is placed in contact with the surface, as in multilayer xerography[30], there is possibility of a transfer of the carrier to the transport state of the dielectric. By careful choice of photoconductor and dielectric characteristics the transfer mechanism can be favored over trapping, or vice versa.[31]

During the time at the surface and during the time spent in the transport states the carrier may be acted upon by a tangential electric field, E_x, causing a lateral displacement.[32]

The field over the surface of a large area of uniform charge is essentially zero and the lines of force lie almost entirely within the dielectric layer.[33] This field provides the force necessary for carrier migration. As the image begins to form, a perpendicular field component, E_z, appears due to the variations in charge density. Likewise, a tangential field component, E_x, begins to form in the plane of the photoconductor. These fields provide for toner attraction during development. The fields are strongest near edges of the charge density difference. (See Figures 11 and 12.) This field would be present in both contact and projection exposures. The direction of the field would depend on the initial polarity of the ASV.

The tangential component becomes stronger as the image forms, but its action on the carriers is to cause lateral motion and attenuation of the image. The result is a lowering of resolution.[34,35] The greater the time delay before trapping, the higher probability of lateral conduction.

For the case where trapping is favored, an image pattern with wavelength λ cannot be resolved unless

$$2B_s u_s T_s E_{po} < \lambda \ .$$

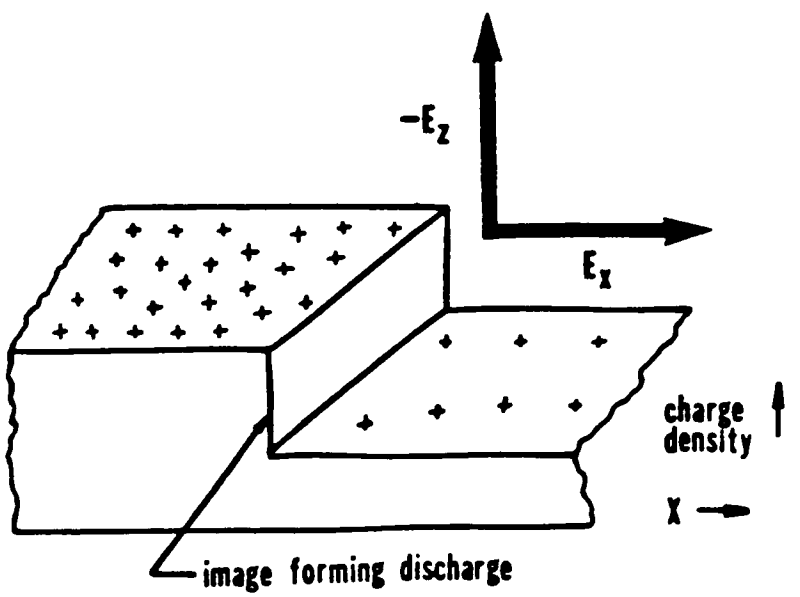

Figure 11. Charge density profile showing discharge due to exposure. (Positively charged photoconductor.)

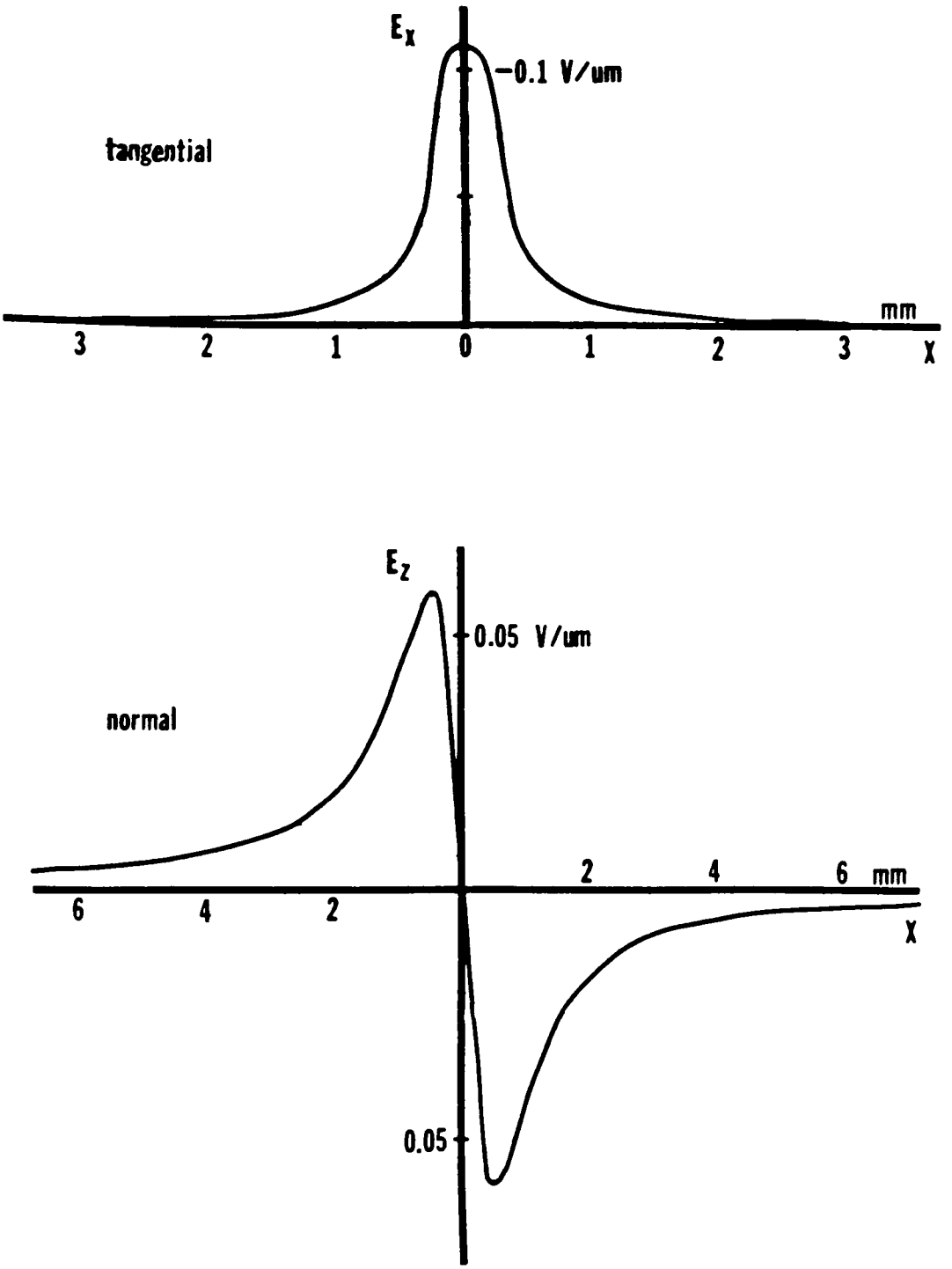

Figure 12. Fields surrounding edge of image after exposure.

where $B_s u_s$ is the surface mobility and E_{po} is the initial field present in the photoconductor.[26]

This means that the mean time, T_c, for a carrier to drift a distance $\mathcal{V}/2$ along the surface is given by

$$T_c = \mathcal{V}/(2B_s u_s E_{po})$$

where $B_s = (1 + \Sigma_i(T_{ri}/T_i))^{-1}$ and T_c is the average of all possible T_t times.

Therefore, as the concentration of slow traps decreases, $\Sigma_i(T_{ri}/T_i)$ will decrease, (T_{ri} will be short for the majority of traps), and the mobility product $B_s u_s$ will be large.

As the mobility increases it can be seen that the time, T_c, for the carrier to drift $\mathcal{V}/2$ decreases and the resolution is lowered

Since the corona charges present on the surface act as slow traps, the lateral motion of the carriers will be significantly reduced. Schmidlin[26,35] reports that the lateral conduction mechanism is not normally present in xerography due to these corona charges except when the photoreceptor is overcoated by an insulating layer prior to charging. In this manner the corona and image charges are separated and the lateral motion at the interface can be large.

In the TEP contact situation the corona charges are located directly on the surface of the OPC and the insulating top layer (i.e. the silver halide original) is usually separated from the OPC layer by a minute air space. This air gap would serve to prevent direct carrier transfer into the target original, promoting trapping.

The system would seem to favor a restricted lateral conduction: low carrier transfer probability and high concentration of slow traps. If the concentration of corona charges on the OPC surface were reduced, however, the mobility of the carriers and the resulting lateral conduction would probably increase.

One mechanism that could affect the charge density on the OPC surface is the possibility of charge transfer to the silver halide material. Transfer of electrostatic images (TESI) is a well known process used in many copier systems[36], and there exists several methods for intentional transfer of charges across air gaps.

While in contact, a corona bias can be applied to the free surface which cause an electrical attraction of the image charges to the receiving sheet[37]. A liquid can be applied between the sheets to cause charge conduction[38]. If the receiving sheet has a conductive backing, the two conductive layers can be connected to a common ground or, if the charges are small, to an external voltage (the voltage causes an external field to drive the charges across the gap).[39]

Spontaneous discharge between sheets in virtual contact can result if the conditions are favorable. These gaseous discharges without an externally applied voltage have received negligible attention.[40]

When a paper is stripped from a photoconductive surface, gaseous discharge can occur due to Paschen breakdown.[41] The Paschen curve (see Figure 13) predicts the breakdown voltage versus the pressure-gap spacing product. The predictions usually fail at small gap spacings due to the dependence on surface conditions and the contributions from field emissions.[40,42]

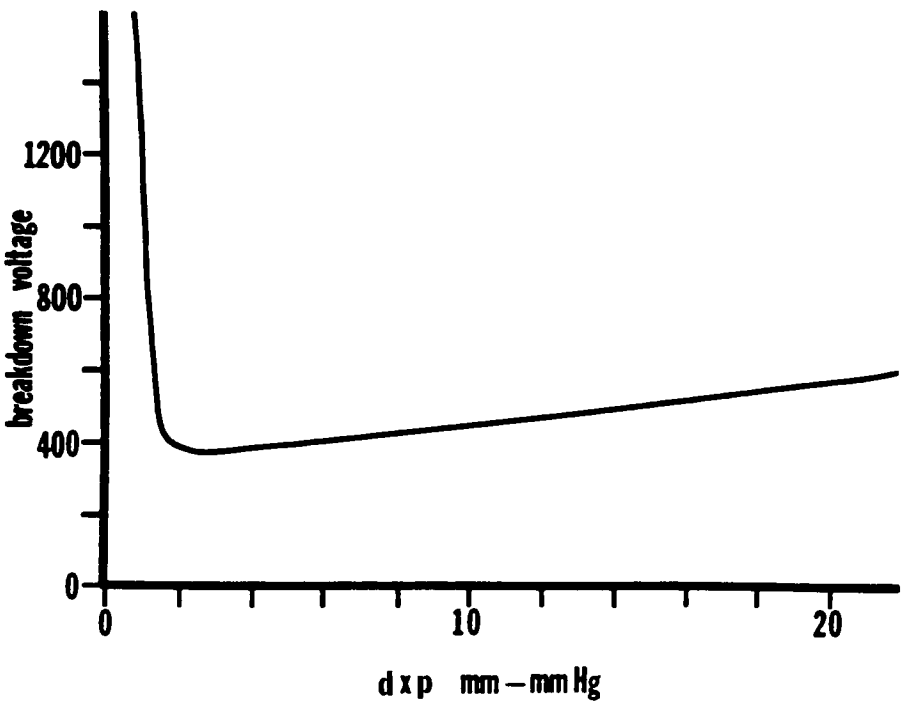

Figure 13. Paschen curve for breakdown of air.

In the case for the transfer of charge from a photoconductive surface to an insulator, as with TEP, the contribution from field emission is probably small.

It can be shown that the field in an air gap resulting from a surface voltage on one of a pair of similar sheets is the same as that of an externally applied voltage of equal size.[43] The transfer of charge from dissimilar sheets, however, is not a simple process but again is probably due to air breakdown.

When contacted, a charge can flow between surfaces to try to equilibrate the potential difference, and upon separation, all, some or none of the charge may remain on the receiving sheet, depending on the conditions.[44] Schaffert[45] gives a possible explanation for this charge transfer mechanism.

Corona produced charges have been shown by experiment to not be tightly bound to the surface, but instead are probably trapped in surface states. A free exchange of charges can occur between two sheets even when the charge initially resides on only one surface. The intimate contact between these sheets under pressure may cause a disruption of the surface states and cause the surface barriers to go to zero.

Theory predicts this to happen for similar sheets but experimentation data has shown a comparable effect in dissimilar materials. If a charge exchange did occur prior to exposure, the lateral surface conduction of the photogenerated carriers in the OPC layer may increase due to separation of these image charges and the slow traps provided by the corona charges. Even if the charge transfer is completely reversed upon separation of the surfaces, the effect of increasing the capture time during exposure would be detrimental to the resolution. Degradation could also result from charges being permanently removed from the photoconductor surface, decreasing the charge gradient in image areas, or from disruptive back transfer during separation.

This charge transfer theory is supported by work done by Weaver, Binns, and Ralston[11,46] who found that charging the original target prior to contact aided the resoltuion transfer. This surface charging would oppose the flow of charges across the interface (see Figure 14).

The interdependancy of the optical and electrostatic effects is evident in the aforementioned material. The air gap present during contact exposure is detrimental to the optical transfer, but decreasing the gap can be shown to promote charge transfer.

Hence, the hypothesis to be tested here is that the loss of resolution during contact exposure is the result of the combined optical and electrostatic effects inherent in the image forming process.

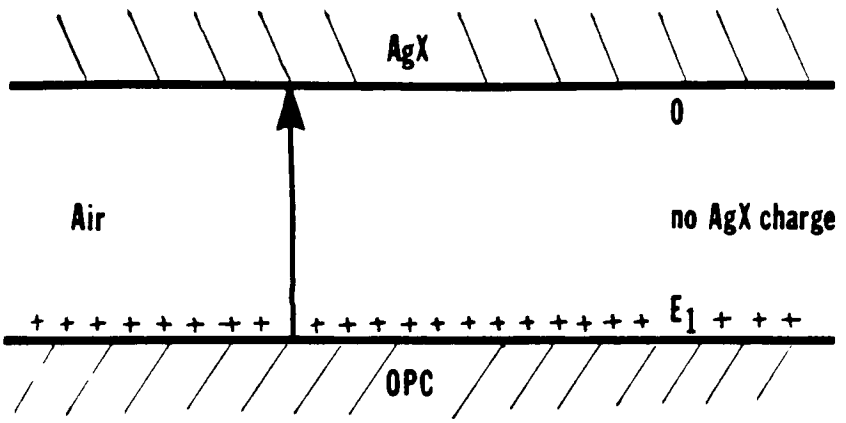

Silver target and TEP film in contact with no charge on target. Result is a field present in films and gap. Positive charging is shown.

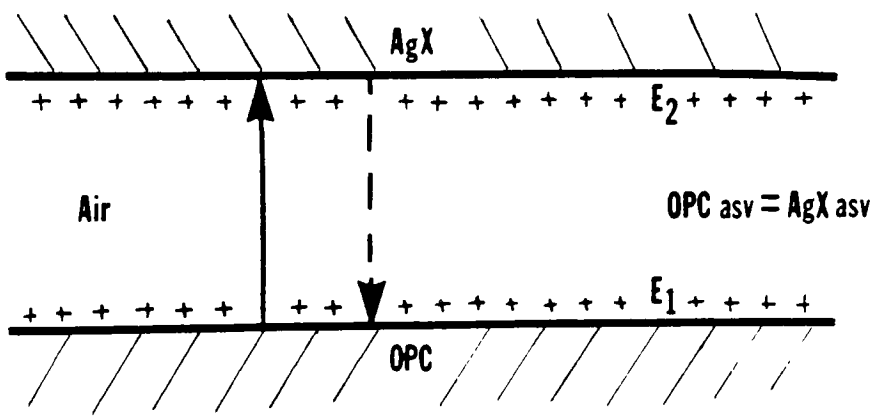

Charge is put onto silver target. Result is lowered field Positive charging is shown for both films.

Figure 14. Effect on field between contacted films when target is charged to same surface voltage as TEP film and with no charge.

II. Experimental

A) Preparation

Preparation for experimentation required the designing of an electrostatic imaging laboratory. This consisted of the collection and construction of various pieces of equipment for the handling and testing of the TEP film:

1. A vacuum plate assembly on which the film is held for charging and developing. This minimizes the handling of the film and prevents any accidental discharge or damage. The plate also holds the film flat during charging and provides a grounded contact. Two sizes of plates were constructed, one to accommodate a full four by six inch fiche and a second to hold a one by three inch sample. The one inch wide sample was used for most of the testing in order to conserve the limited supply of film and toner available. (See Figure 15.)

2. A Scorotron charging unit. An automatic charging device was designed to produce a uniform surface voltage of up to -1200 volts. The device had to meet certain citeria for optimum uniformity [47]: a screen controlled corona charging assembly (Scorotron) with a screen/film gap spacing between 0.125 and 0.060 inches to prevent streaking or arcing, an input corona voltage of 6 to 8 kilovolts D.C., an adjustable screen voltage to give a corona/screen voltage ratio of 6:1 for best results, and an adjustable plate transport speed for variable charging rates.

The Scorotron charging unit was constructed of a Plexiglas frame mounted on two micrometer heads for adjusting the unit height above the film. Three tungsten corona wires are spaced 3/8 of an inch apart

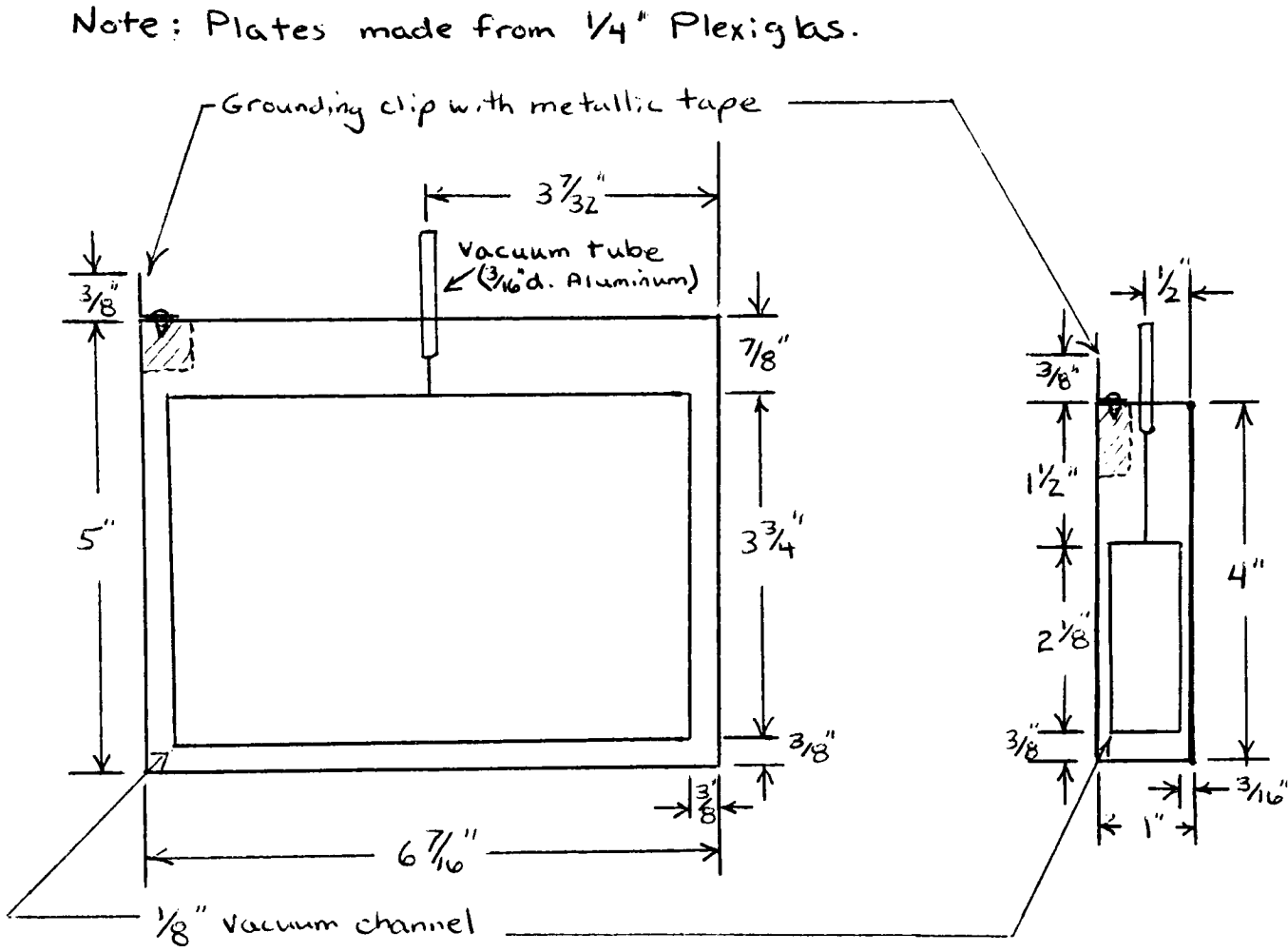

Figure 15. Vacuum frame construction (1/2 scale).

and are mounted in the center of the frame, 3/8 of an inch above the screen wires. The screen consists of a series of tungsten wires running parallel to the corona wires and spaced 5/32 of an inch apart. (See Figure 16.) The Scorotron charging unit was powered by two independent power supplies: a Sola Electric model 52-017-7 high voltage supply with a -6.5 KV output with a 1.0 mA maximum current, and a Trek Corporation model 605 variable high voltage supply (0 to 1 KV) with a 1.0 mA maximum current. The charging rate of the film could also be controlled by varying the current of the corona supply. (See Figure 17.)

3. An electrostatic charge measurement device. An electrostatic probe was incorporated into the charging device to provide immediate post-charge apparent surface voltage (ASV) measurement. The output from a Monroe model 138s-4 Feedback Electrostatic Voltmeter was attached to a Beckman Electrograph-Polarograph modified for use as a strip-chart recorder for measurement of initial ASV and the dark decay rate. The measurement apparatus was also used to examine the uniformity of the surface charge on the film. Measuring capability of the system in the 0-2000v range was ± 10v.

4. An exposing source. A high output tungsten source with a focal plane type shutter was modified with optics to produce a collimated exposing system. A 200 watt, 6.6 A General Electric tungsten-halogen bulb was placed so that the filament was at the focal point of a 65 cm lens with a diameter of 12 cm. This arrangement provided for uniform collimated illumination of the film sample. The film samples were exposed in a vacuum frame located 80 cm below the collimating lens. Shutter times available for the exposure ranged from 0.05 to 60 seconds. (See Figure 18.)

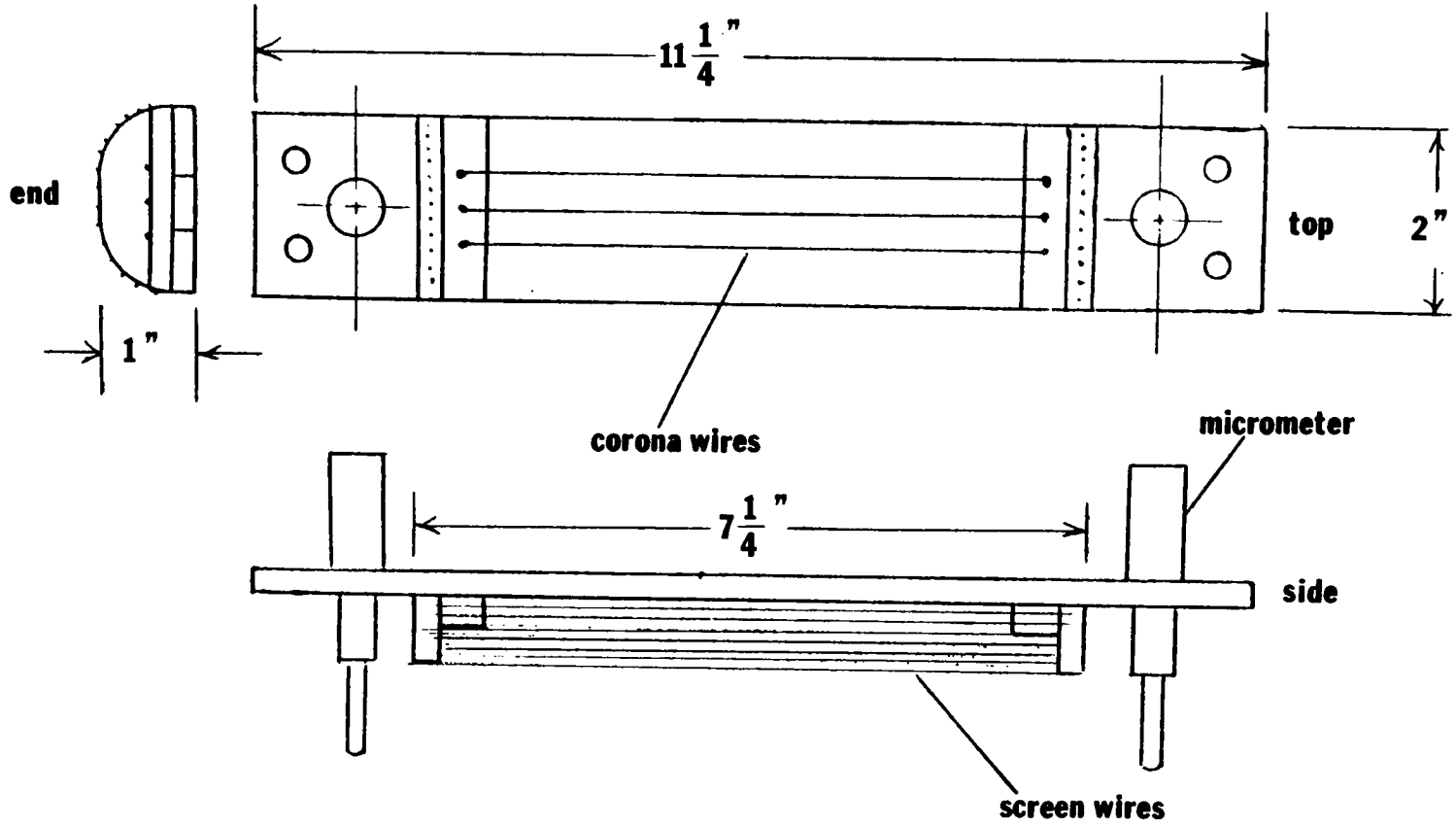

Note: Full description of assembly is located in the text. See Appendix I for a full set of Scorotron drive unit drawings.

Figure 16. Diagram of Scorotron charging assembly (1/2 scale).

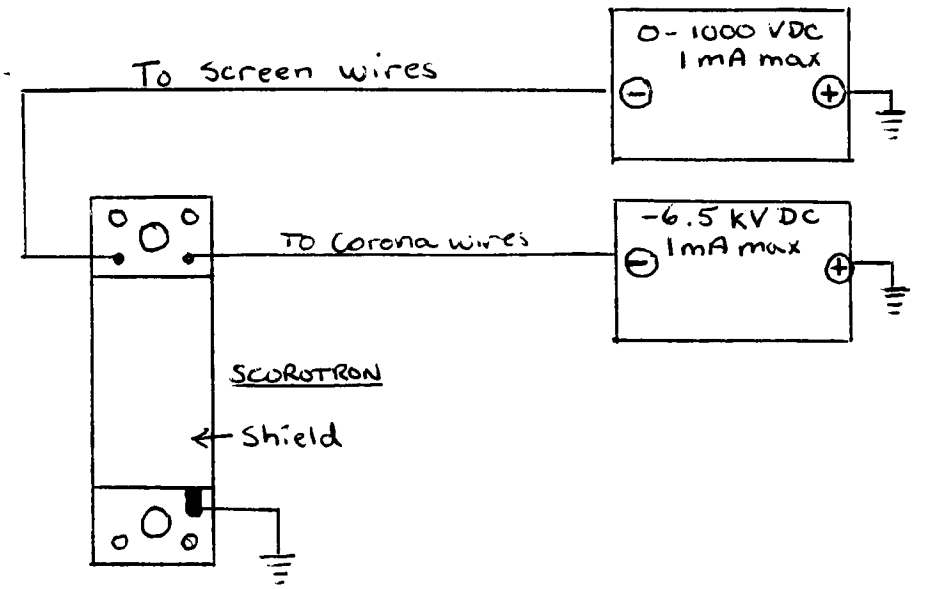

Figure 17. Electrical connections for Scorotron assembly.

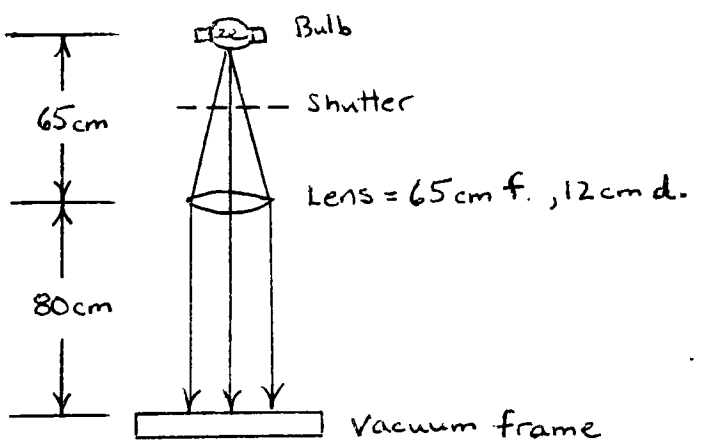

Figure 18. Exposure system characteristics.

5. A developing apparatus. A Plexiglas dip tank was constructed to accommodate the four by six inch film/plate assembly and a development electrode. The electrode had to be held in close proximity (0.035 to 0.050 inches) to the film surface during processing for optimum uniformity.[47] This was accomplished by mounting plastic spacers on the edges of the development electrode. The electrode itself was constructed of a piece of copper-clad epoxy board with one side etched away and was attached to a Trek model 605 variable high voltage supply.

A second development apparatus was constructed to match the one inch wide plate. The tank for the small plate was made from a piece of 1-3/8 inch diameter PVC pipe mounted on a Plexiglas base and had a one inch wide development electrode designed as above. (See Figures 19 and 20.)

B) Testing of Equipment

After preparing the laboratory, the equipment was tested for uniformity and repeatability. Techniques were practiced and adjusted until repeatable so that the results of the experiments could be attributed solely to the mechanisms being studied. Both latent and developed images were examined:

Surface charge uniformity was measured by passing the charged film/plate assembly beneath the probe of the electrostatic voltmeter in both directions across the width of the film and recording the result on a strip-chart recorder. This was done 30 seconds after charging.

Charged and developed film was examined for streaking, mottling, and point discharging visually and by densitometer. The developer and film being used for this initial testing are James River Graphics type T18-18 developer and P4-005 film. (See Appendix A.)

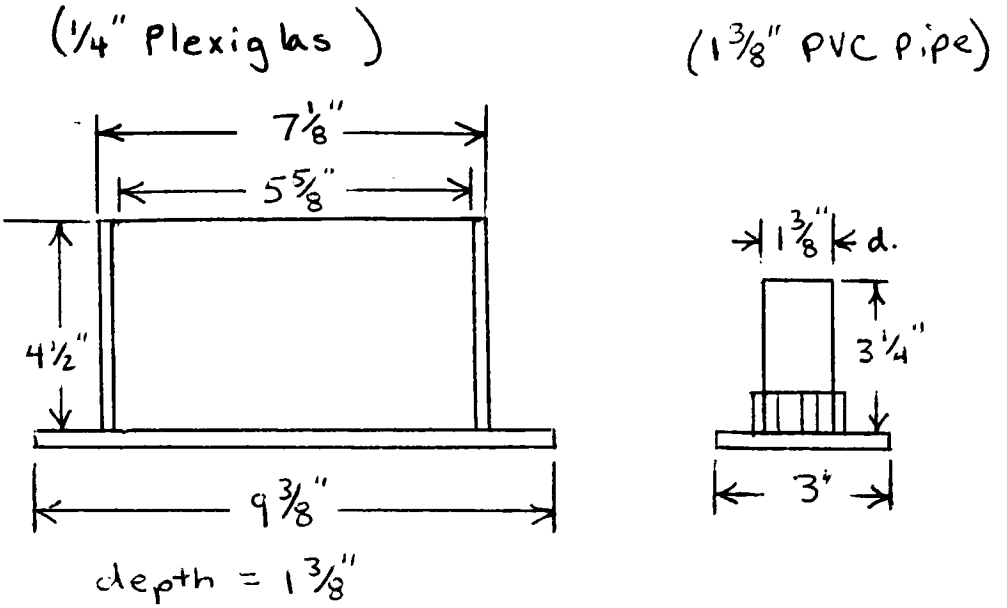

Figure 19. Film development tanks. (For 6 and 1 inch fiches.)

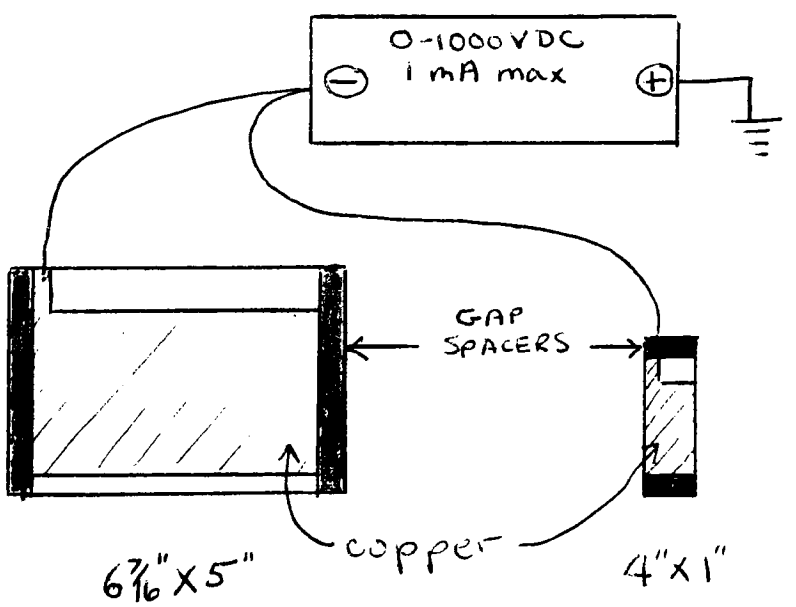

Figure 20. Development bias electrodes. (For 6 and 1 inch fiches.)

It was found that the film edges were not evenly charged due to the finite size of the charging wire assembly; however, the central area of the film was satisfactory for use in the experiment. (See Figures 21 and 22.)

C) Film

The film used for the experiment is James River Graphics type P5-003. (See Appendix A.)

The nominal ASV of -960 volts was obtained with a corona voltage of -6.5 KV at 0.3 mA and a screen voltage of -900 volts at 1.0 mA. The plate transport speed for this ASV was one inch per second.

The delay time between charging and exposing was kept constant between 45 seconds and one minute. The dark decay rate for this film was measured under safelight conditions and is shown in Figure 23.

D) Preparation of Experimental Developer

An experimental version of the T18-18 electrodeveloper designed by James River Graphics has been chosen for use in this experiment. The developer, T48-5K, is not commercially available and so must be prepared as needed. The method of preparation was obtained through a training session at the James River Graphics research facility in South Hadley, MA.

A developer concentrate was diluted volumetrically with Isopar-G[48] to an 18.5% transmittance. The volumetric calibration was determined with a Bausch and Lomb spectrophotometer at 575 nm in a flow-through cell, according to standard procedures used at James River Graphics.

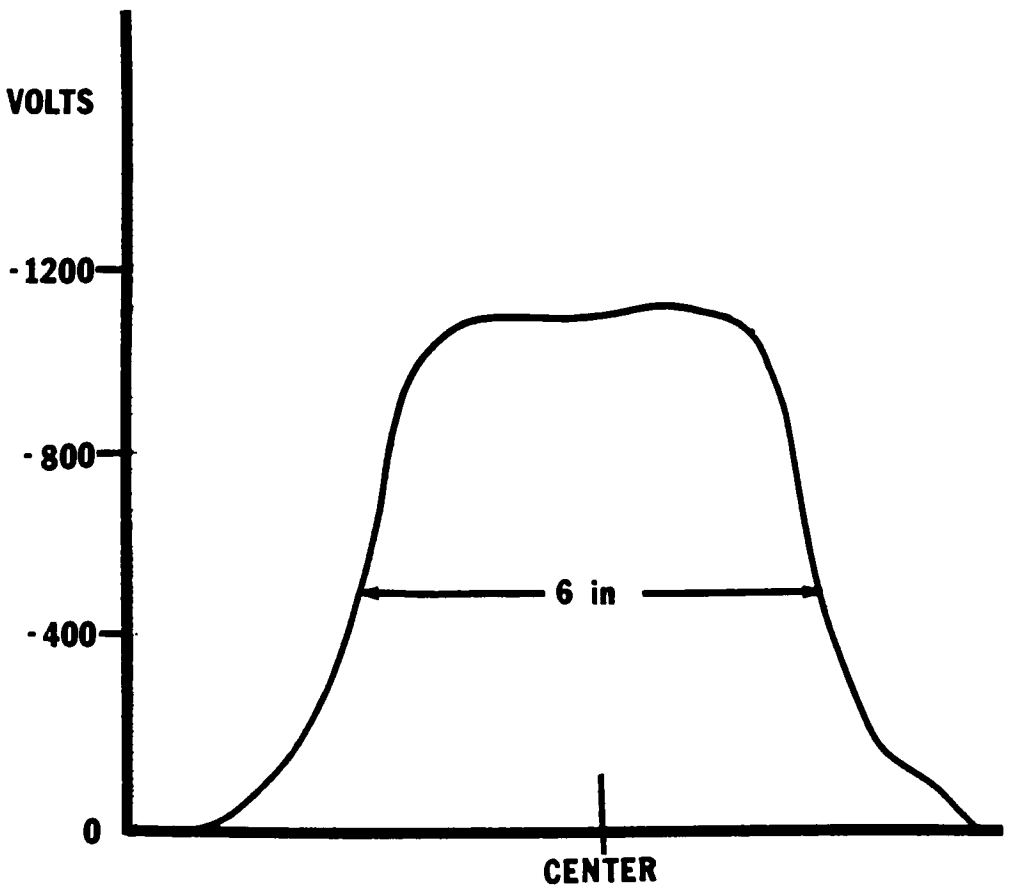

Figure 21. Cross field uniformity of charged TEP film. 4X6 inch fiche scanned perpendicular to direction of charging (parallel to charging wires).

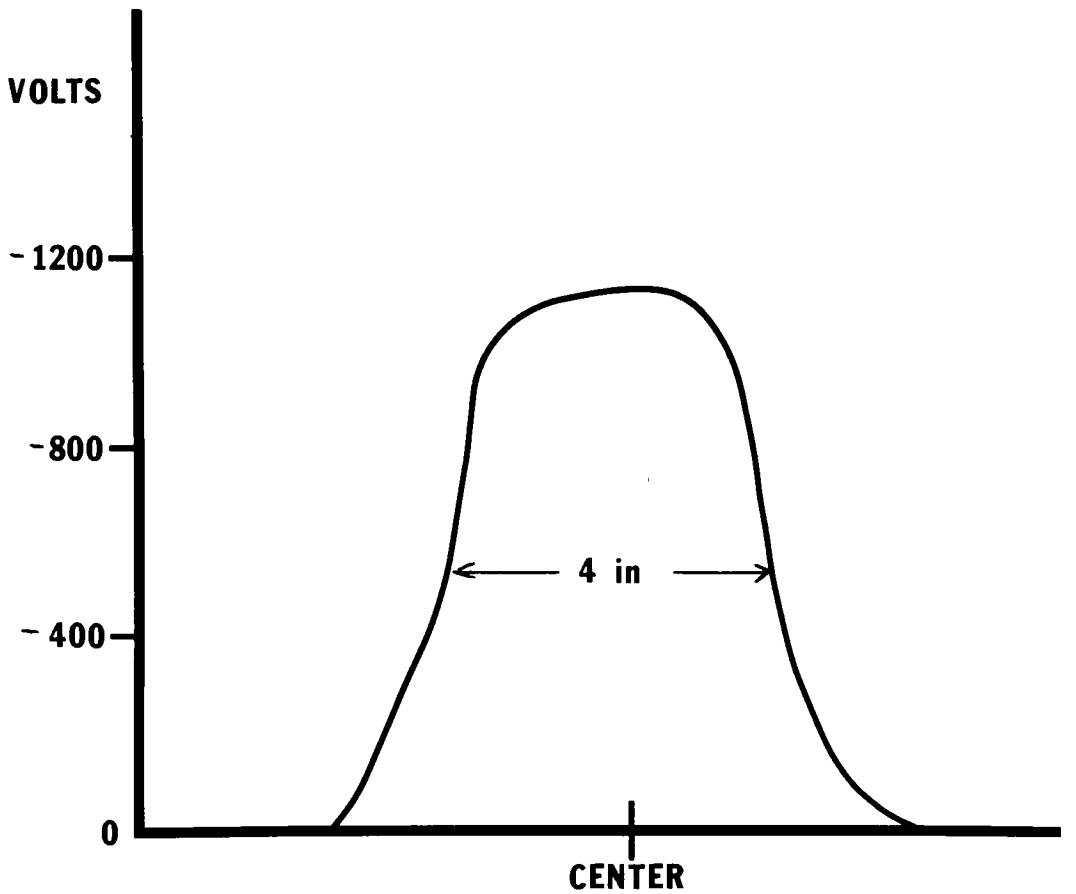

Figure 22. Cross field uniformity of charged TEP film. 4X6 inch fiche scanned parallel to direction of charging (perpendicular to charging wires).

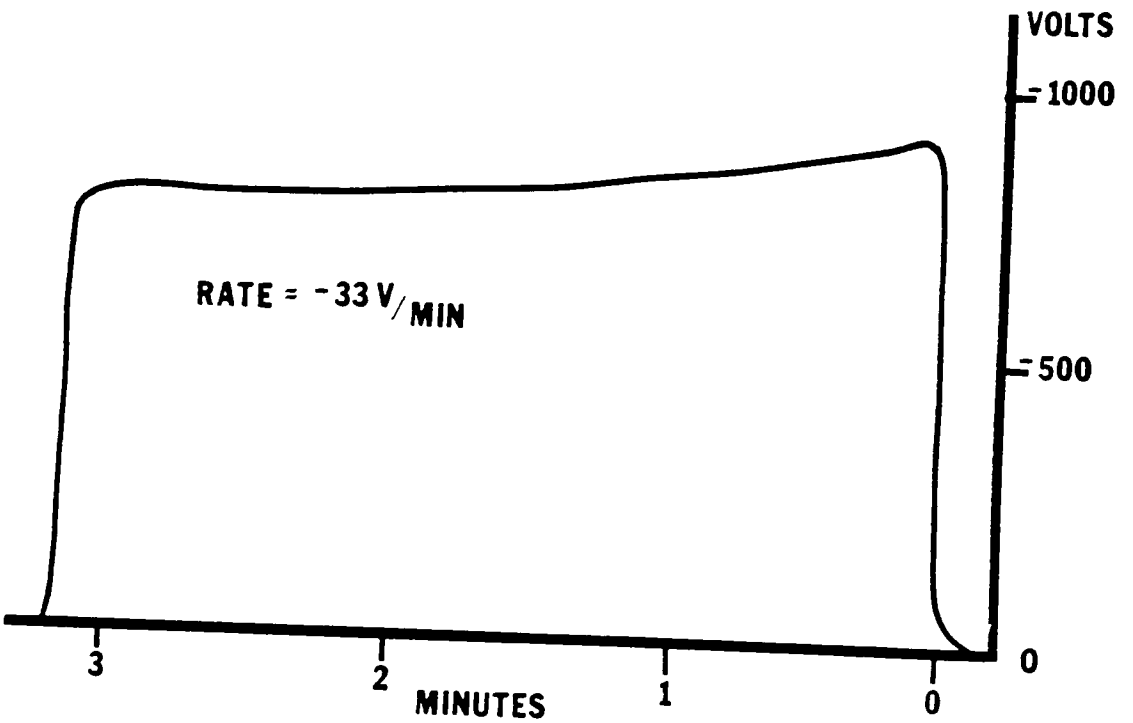

Figure is copied from the original strip chart record, hence it is reverse reading due to the direction of scan. Center of film was used for measurement. Performed under safelight conditions.

Figure 23. Dark decay of P5-003 TEP film (-960V initial charge).

E) Processing Procedure

The TEP film was processed according to the procedures listed in the James River Graphics report "Transparent Electrophotographic (TEP) Process, Manual Processing Procedures".[47] This manual provides a standardized procedure for laboratory processing of the film. An outline of the basic procedure is given in Appendix C.

All samples were processed to an average gradient ($\bar{G}$) of 1.0. (See Appendix B.) The gradient was controlled by varying the development electrode bias potential. For a positive system, the type used in this study, the bias voltage is set to the same polarity as the TEP ASV. A sample bias voltage vs $\bar{G}$ graph is shown in Figure 24 for the test film P4-005. Adjustments for $\bar{G}$ for the P5-003 film were made in the same manner.

F) Experimentation

1) Silver-halide target comparisons

The silver-halide targets used during this project were prepared by contact printing a high resolution chrome-on-glass, tenth-root-of-ten progression target onto a variety of films. The TEP film/developer combination used in this study is designed to yield a maximum resolution of about 300-400 lp/mm, so the prepared silver-halide targets were required to have resolution limits well in excess of these frequencies. The films were processed to a final image contrast between 6:1 and 9.5:1. The granularity and Callier Q factor for all targets was measured using an Ansco model 4 microdensitometer.

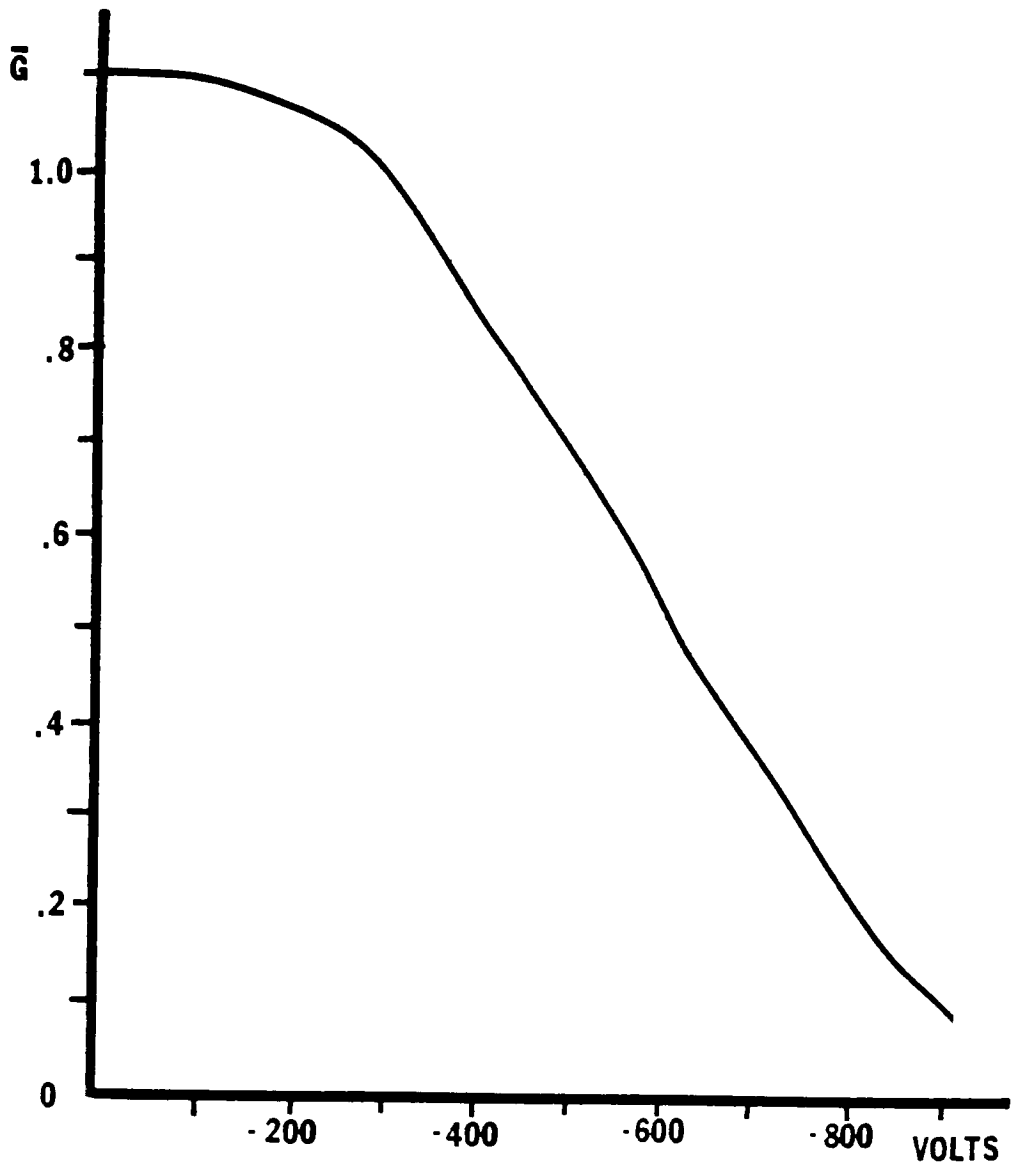

Film shown here is P4-005, the initial test film used in the preliminary part of the study. A complete curve for P5-003 was not generated, but the trends are similar.

Figure 24. Sample plot of $\bar{G}$ vs bias voltage during development.

Target contrast was determined by scanning the 100 lp/mm element of each target at 100X magnification with a 0.25 mm diameter circular aperture. Granularity was measured at a diffuse density of about 1.0 with a 0.5 mm circular aperture and a magnification of 100X. The granularity is reported as 100 times the standard deviation of the density fluctuation. The Callier Q factor was determined by measuring a step tablet exposure specularly in the Ansco microdensitometer and diffusely on a Macbeth TD-500 densitometer. The ratio of $D_{specular}$ to $D_{diffuse}$ at a diffuse density of about 1.0 gives the Q factor. Target characteristics are given in Table 2.

Six replicates were made on each of the four targets with contrasts between 6:1 and 7:1. Exposure times were varied to give approximately the same target density on the TEP film. Resolution was measured visually under 200X to 400X magnification by the experimenter.

2) Precharging of silver halide targets

In order to test the effect of charge transfer, exposures were made onto the TEP film using the Copex Pan resolution target original charged to a variety of ASV's ranging from zero to an ASV greater than that of the TEP film. The time lapse between charging and exposure for the TEP film was about one minute. The silver halide surface charge was controlled by varying the screen potential between zero and -900 volts.

The decay rate for the silver halide target was rapid, (see Figure 25), so the time between the charge measurement and exposure was kept to a minimum; about 15 seconds.

Target	Ddiffuse	Dspecular	Contrast	Q	RMSG
SO-173	1.17	1.29	6.9:1	1.10	0.102
649-F	0.98	1.15	6.3:1	1.17	0.130
EK-3414	0.93	1.18	6.0:1	1.27	0.128
Copex Pan	0.91	1.19	6.6:1	1.31	0.162

Table 2. Silver halide target characteristics.

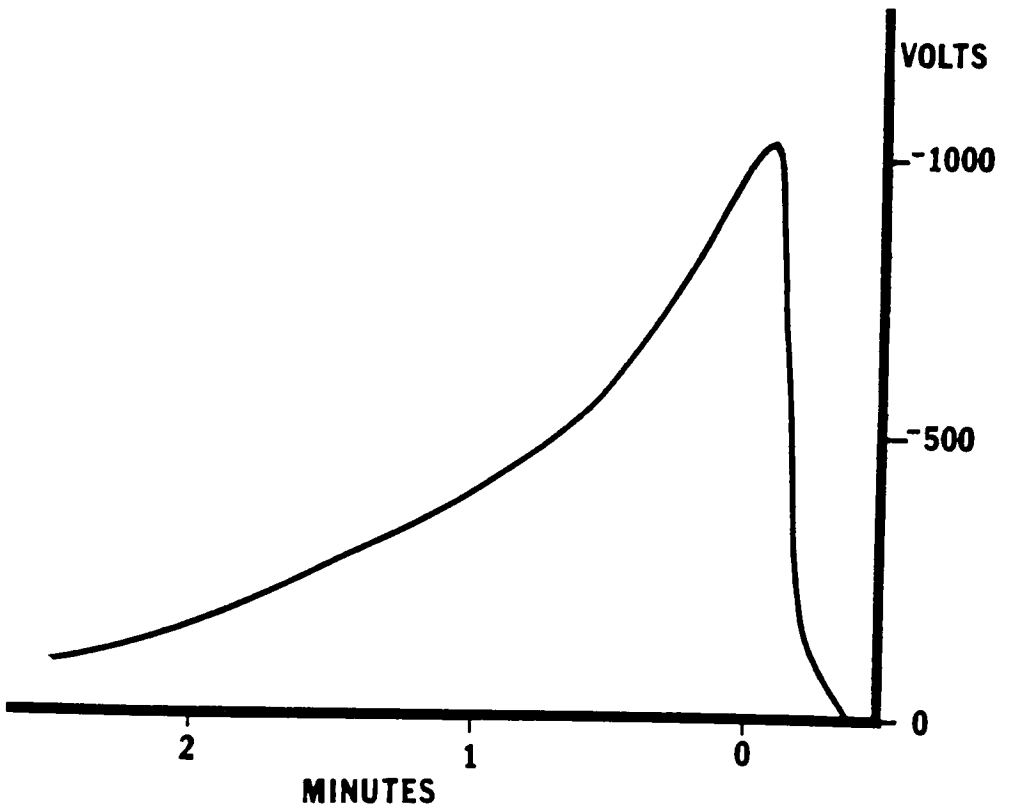

Rate is approximately 500 V/minute for the first minute. Figure is copied from the original strip chart record, hence it is reverse reading due to the direction of scan. Copex Pan target used for test.

Figure 25. Dark decay of charged silver halide target.

Due to this rapid decay, an accurate measure of any electrostatic charge transfer was not possible, only the effect on resolution could be observed. Four replicates at five different levels of charge were run while keeping the TEP surface charge constant.

3) Water content of silver halide target

The effect of the water content of the original silver halide target when used in the contact situation was investigated to determine if any conductive discharge occurs. A 649-F (9.5:1) target was allowed to equilibrate in a variety of relative humidity environments before contact exposure.

Saturated salt solutions were placed in a sealed glass chamber along with the target and a relative humidity meter. For the lowest %RH a dessicant replaced the salt solutions. A list of the salts and the dessicant is given in Table 3. Ambient conditions were measured with the same meter.

The target was given approximately one hour to equilibrate each time it was introduced into a new environment. This time was necessary to allow the film base to fully equilibrate.[50] Subsequent times after each exposure for the same environment was only 15 minutes since the gelatin requires only a few minutes to regain its water content.[50] Little change in the film base would occur during the short exposure period, so a shorter equilibration time was adequate.

4) OPC thickness

Two variations of P5-003 film with coating weights

Salt	Approximate %RH	Temperature
K_2CrO_4	87%	28°C
$Na_2Cr_2O_7 \cdot 2H_2O$	72%	28°C
Ambient conditions	52%, 65%	25°C
$LiCl \cdot H_2O$	36%	27°C
$CaCl_2$ dessicant	22%	25°C

Table 3. Saturated salt solutions for constant humidity chamber.

higher and lower than the normal weight were provided by James River Graphics to determine the effect of OPC thickness on resolution. Coating weights of 1.32 and 2.52 $lbs/10^3ft^2$ were provided and the normal P5-003 coating weight was determined experimentally. The OPC layer of a sample of normal film of known dimensions was first washed off the base using methyl-ethyl ketone. The methyl-ethyl ketone was then allowed to evaporate in a drying oven. Differential weighing gave a coating weight of 2.02 $lbs/10^3ft^2$.

A 649-F target was used to generate 11 replications on each of the three samples. Charging current, exposure time, and development bias potential had to be altered to obtain identical sensitometries for the different films. These characteristics for each film are listed in Table 4.

5) Microcamera exposure of TEP

A microcamera system was designed to test the projection imaging capabilities of the TEP film. The slit illumination system of an Ansco model 4 microdensitometer was modified for use as a projection exposure camera. The slit assembly was replaced by the silver halide target and a shutter was placed between the lamp and the target. A diagram of the system is shown in Figure 26. The film is held in place by a vacuum plate with a 5/8 inch hole in the exposure area. This hole allowed for the viewing and focusing of the projected image with the aid of a second microscope system behind the plate.

The objective used in the system was a Zeiss Epi-plan 16X 0.30 NA microscope objective. The theoretical cutoff frequency for this lens for a line image is 1100 lp/mm.[51] The system magnification with this objective is 0.125X or a 8X reduction.

Film coating weight	Charging current	Developer bias	Exposure time
1.32 $lb/10^3 ft^2$	0.4 mA	-500 V	0.6 sec
2.02 $lb/10^3 ft^2$	0.3 mA	-500 V	0.4 sec
2.52 $lb/10^3 ft^2$	0.3 mA	-300 V	1.0 sec

Table 4. OPC coating weight process parameters.

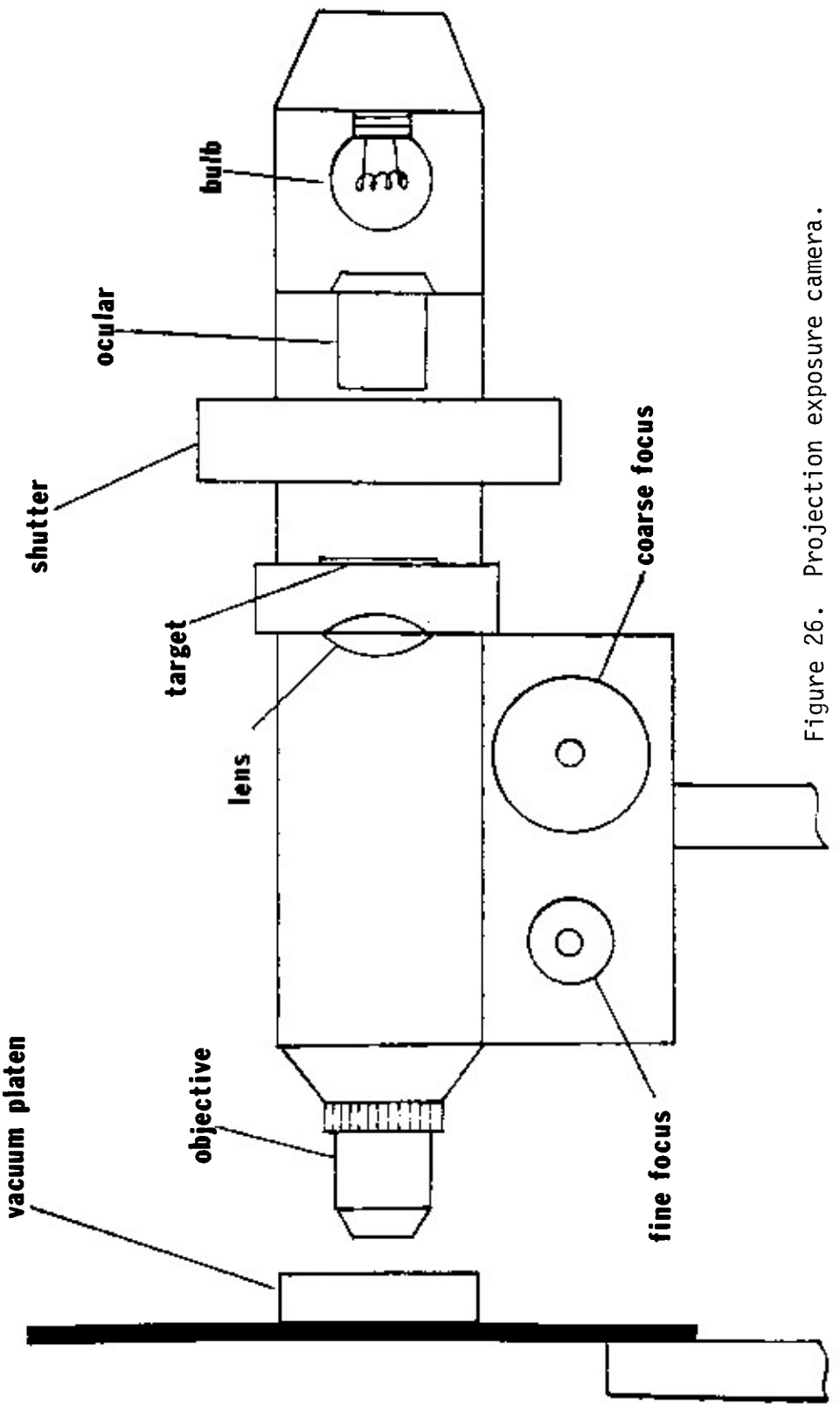

Figure 26. Projection exposure camera.

The lamp was powered by a Sorenson 0-40 V dc power supply. The output illuminance was varied by changing the bulb current. Bulb voltage was limited at 3.5 V. Exposure time was constant at 0.01 seconds.

Two different targets were used, a 6.0:1 649-F target and an 11:1 SO-173 target. A through focus and exposure series was used to find the optimum projection resolution. The focusing increment used was 2.5 um and was adjusted using the fine focus knob of the microscope system. Initial coarse focus was accomplished by first using the viewing microscope system to focus on the surface of a developed piece of TEP film and then adjusting the target focus to the same image plane.

6) SEM observations

Observations of electrostatic latent images were made on two scanning electron microscopes, an International Scientific Instruments (ISI) TV Mini-SEM and an ISI-40 SEM.

The TV Mini-SEM operated with an accelerating voltage of 10 KV and an emission current of 120 uA. The sample holder allowed for a sample approximately 1/2 inch square. Total time between exposure and viewing was about 5 minutes. Although magnifications of up to 20,000X were available, the high accelerating voltage caused too rapid a degradation of the viewing for useful observations.

The ISI-40 instrument operated with a tungsten filament at a 2 KV accelerating voltage and an emission current of 90 uA. This enabled much longer scan times with less degradation of the images. The time between exposure and viewing in this case was approximately 15 minutes due to the necessity to transfer the exposed sample to another building where the ISI-40 was located.

In order to obtain the best results on this instrument, an experienced operator was used in this part of the experiment.

The samples were prepared as for the developed images and mounted with Scotch tape on the sample stubs. The samples were not metallized. Photographs were made off the TV monitor of the Mini-SEM using a 35 mm camera with a 100 mm macro lens. The ISI-40 provided a built-in Polaroid camera system. Viewings and photographs were made at both different tiltangles (angle of speciman relative to beam) and magnifications. Beam current was decreased at higher magnifications to reduce the amount of charging of the sample. The effect of charging was to destroy the latent image.

7) Data collection

Data collection was performed as randomly as possible to comply with the requirements of the statistical methods being used. In the case of the study of water content of the silver halide target the experiment was not completely randomized.

The levels of chamber humidity, resulting from a different salt or condition, were randomized before starting data collection. The original intent was to perform four replicates at each level.

For the salt solutions, however, the chamber humidity, the independent variable, was not the same for each replicate at each level. The decision was to treat the data not as structured replicates but as separate levels of the independent variable.

Due to the time required to prepare and equilibrate the chamber, these four samples at each condition were done in sequence instead of completely randomizing the design. The implication of this is to add the

possibility of a time dependence on the data, (i.e. the resolution may be a function of both the time it was run and the humidity of the chamber).

Since the original levels of chamber humidity were randomized, the effect of this time dependence is not as severe as it would be had the samples been collected in a more deliberate pattern. The result of this collection method on the analysis would be to cause an underestimation of the error term or overestimation of the response variable. (See Appendix E.)

Analysis of resolution results for all parts, except the SEM observations, was done with a Bausch and Lomb stereo microscope under magnifications of 100 X to 430 X, as required.

Sensitometric analyses were done by contact exposing a Kodak #2 step tablet onto the TEP film under the same source as used for resolution exposures. Illuminance was constant at 1800 lux and exposure time was adjusted for the various conditions used. Density readings were made on a Macbeth TD-500 densitometer.

Resolution of the electrostatic latent images viewed under the SEM was determined visually by examining the photographs taken from the monitor screen. (See Appendix G.)

III. Results

A) Silver Halide Target Comparisons

Average resolution and 95% confidence intervals are plotted against granularity, (σ_D), and Callier Q factor in figures 27 and 28. On the average, the highest resolution is reported for the 649-F target, the lowest for the EK-3414. (Average was computed using six samples.)

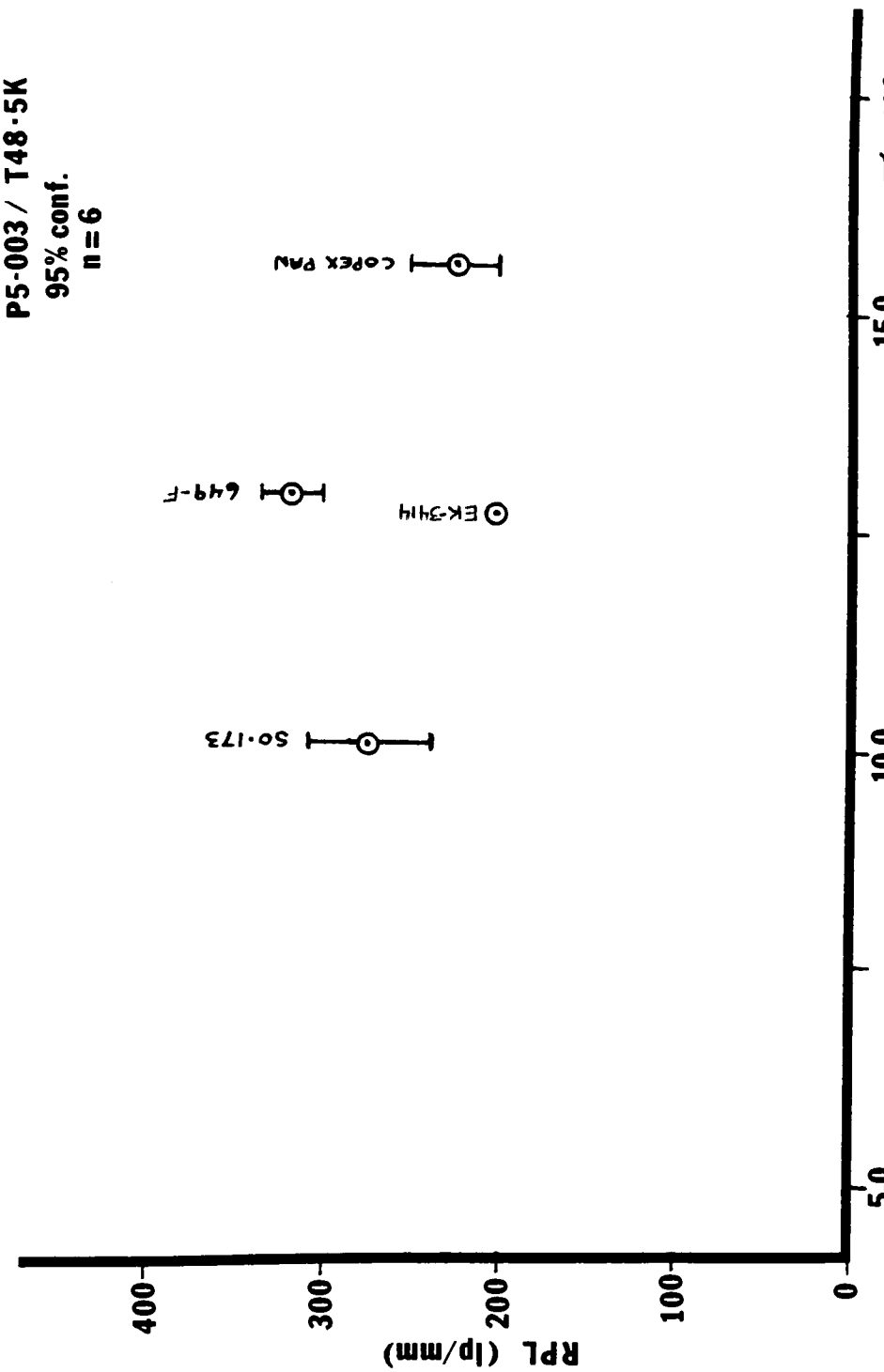

Figure 27. Resolving power limit (RPL) vs σ_D of target. P5-003 film used with T48-5K developer.

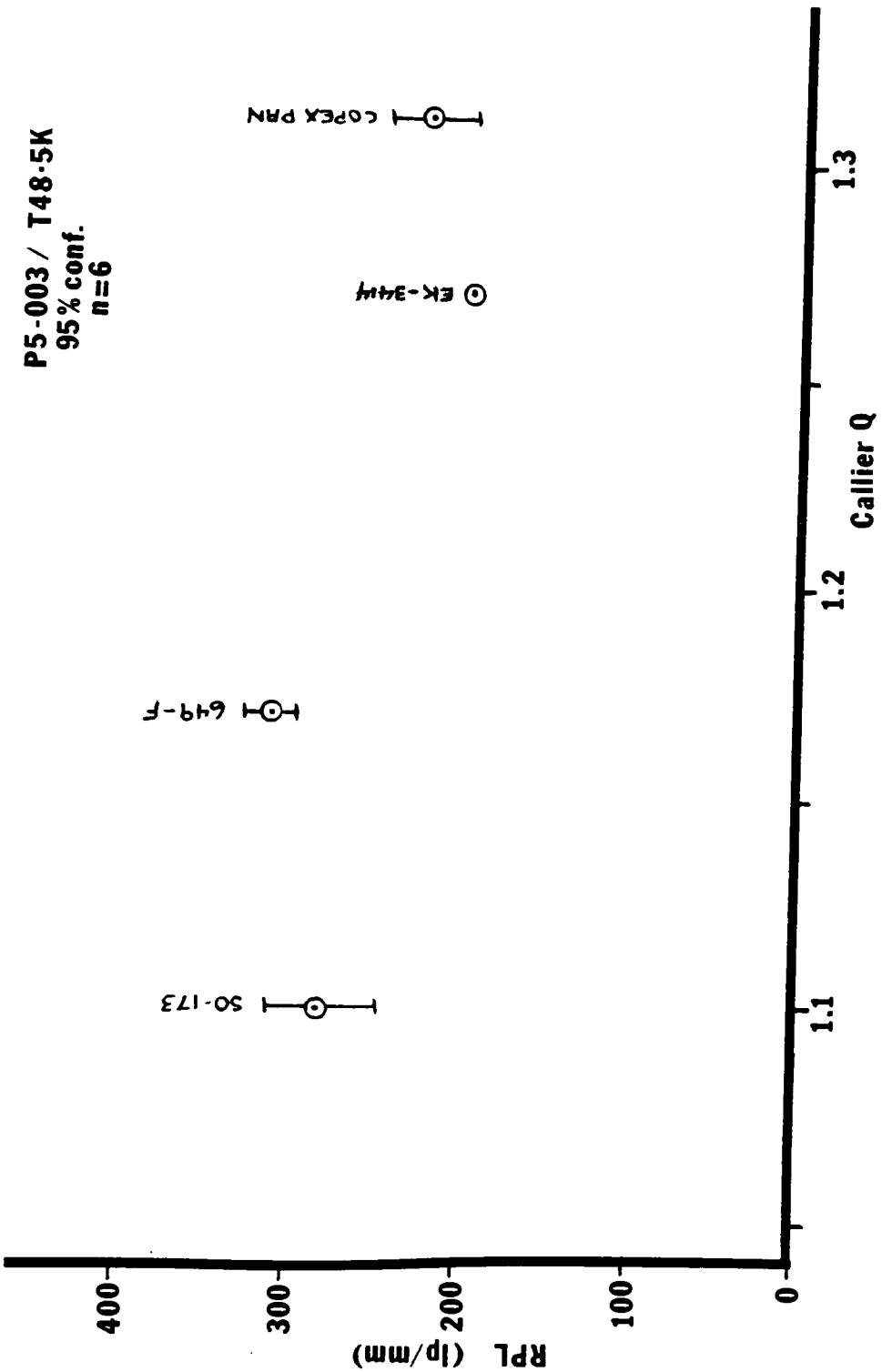

Figure 28. Resolving power limit (RPL) vs Callier Q factor of target. P5-003 film used with T.48-5K developer.

A Kruskal-Wallis test for independence was run on the data to determine if there was a significant difference in the results due to the type of target used. (See Appendix D.) The hypothesis that all the population distributions for the four targets are the same was rejected with greater than 99% confidence. Multiple comparisons were run on the data to determine which samples differed from the others. (See Appendix D.) Results of the comparisons showed that the four sets of data were from four independent populations with 95% confidence. The closest of the comparisons was between the 649-F target and the SO-173 target.

If the confidence level is increased to just over 97%, the difference between the two targets is no longer significant. The same is true for the EK-3414 and the Copex Pan targets. This would indicate that at a 97% confidence level only two populations are present.

Although the EK-3414 target had a resolving power limit, RPL, in excess of 800 lp/mm, resolution above 200 lp/mm could not be obtained on the TEP film. The lines and spaces of the bar target were sharp at the 200 lp/mm level, however, the clear bars were beginning to break up with intermittant dark blotches. At the higher frequencies the bars were almost completely broken up by these dark blotches.

It is believed that these dark areas are due to the silica particles used on the base side of the film. These matte particles are necessary when the film is used as an aerial film to reduce handling problems and reaction between layers of the film, but this coating appears to hinder this type of contact duplication.

B) Charging of Silver Halide Targets

An 11:1 contrast Copex Pan target was charged to five levels of surface voltage between 0 and 1073.5 volts. The surface voltages reported are averages of the four replicates for each level. Results are shown graphically in Figure 29.

A Kruskal-Wallis test was performed on the data to test for differences in the means of the populations for the five levels. The hypothesis that all five samples were from the same population was rejected with greater than 98% confidence. This indicates that the charging of the silver halide target causes a difference in response for at least one of the five levels.

To determine which levels are different, multiple comparisons were made between the levels. At a 95% confidence level the test shows no significant difference between the 0V, the -410 V, and the -774 V levels. Likewise, no difference was found between the -969 V level and the -1073.5 V level. A significant difference does occur between the former and latter groups. Charging at or above the magnitude of the surface voltage level of the TEP film, at the same polarity, does appear to yield significantly higher observed values than the other voltage levels, including no charge.

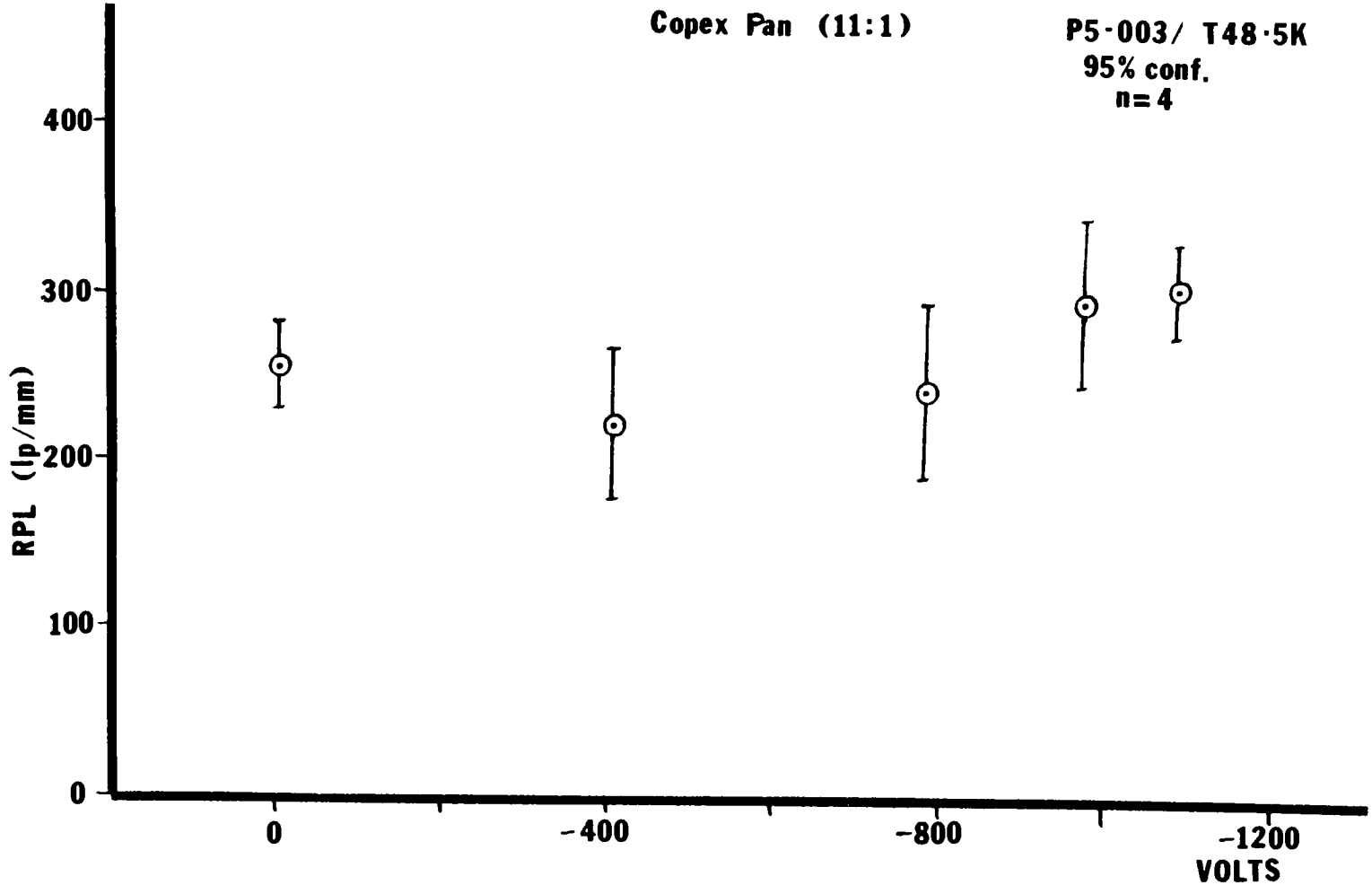

Figure 29. Resolving power limit (RPL) vs surface voltage of charged silver halide target. P5-003 film used with T48-5K developer.

C) Water Content of Original Target

Twenty-three tests were run at levels of relative humidity between 18% and 88%. A plot of resolution limit vs % relative humidity of target is shown in Figure 30.

The highest %RH samples (>80%) showed signs of sporatic discharge in the form of clear blotches over much of the target area. At these levels the moisture content of the gelatin is greater than 12%.[52]

An analysis of variance (ANOVA) was run on the data using a first order regression model (See Appendix E). The test gave a significant regression with a confidence level greater than 99%. This indicates that there is a significant negative correlation between the %RH and the observed value of resolution limit. The regression model for this data was:

$$RPL = 301.1997 - 1.0211(\%RH)$$

A second analysis was run using a Cox and Stuart test for trend. (See Appendix F.) The null hypothesis here is that no negative correlation is present in the data. In this test the %RH values are ordered and the last eleven observations are paired with the first eleven; the twelveth observation is omitted.

The test statistic is the number of pairs of observations in which the second value exceeds the first. This shows whether the higher values of %RH yield lower values of resolution.

The results of the test indicate that there is negative correlation at confidence level greater than 98%.

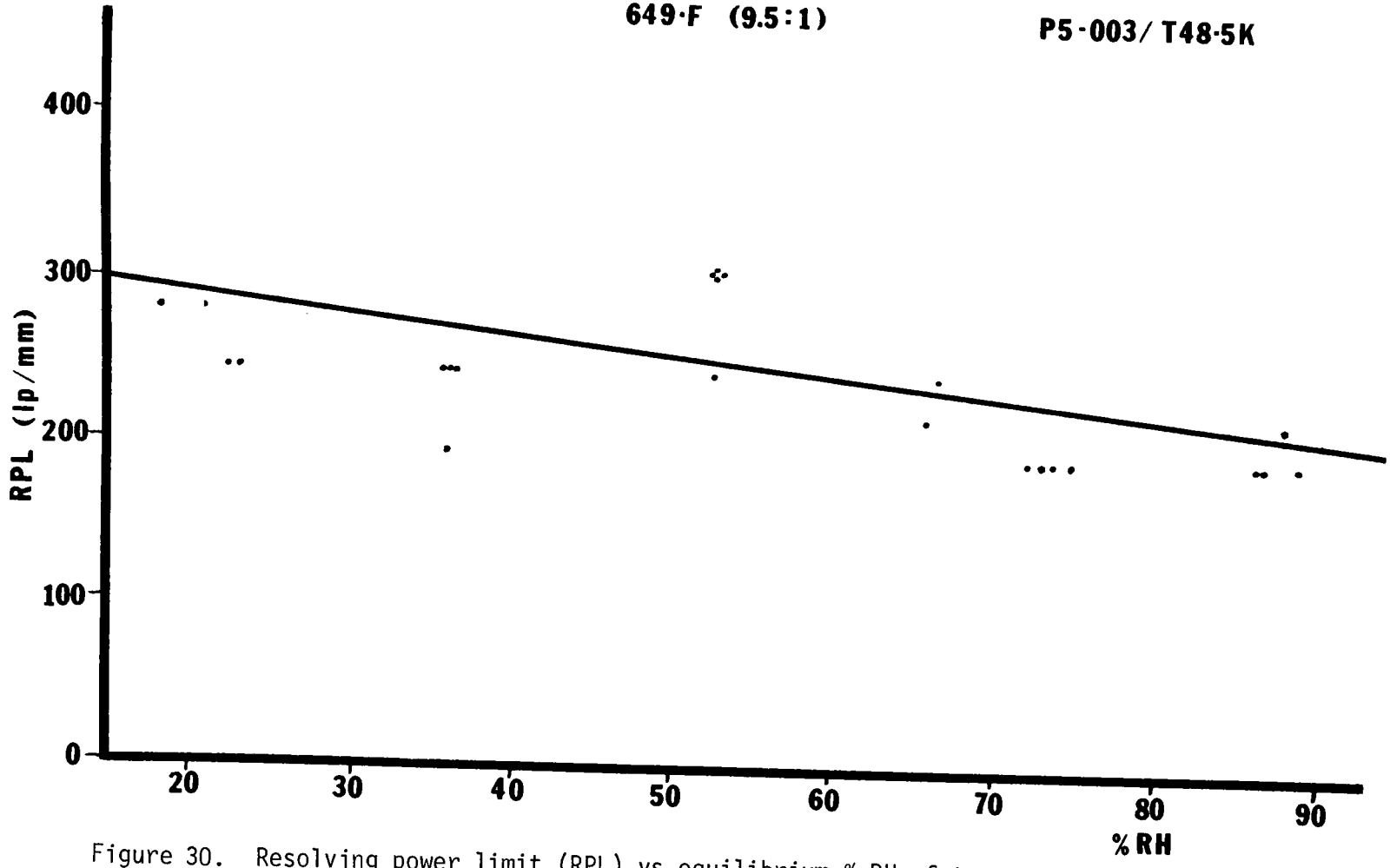

Figure 30. Resolving power limit (RPL) vs equilibrium % RH of target. P5-003 film used with T48-5K developer.

D) Thickness of OPC Layer

Eleven samples at each of three levels of coating weight were run on the film using a 6.3:1 649-F target. Increased or decreased coating weights result in increased or decreased OPC layer thickness, respectively. This means a change in the path length over which the exposing photon may travel laterally before being absorbed. (See Figure 4.) The average depth of absorption, X_3, will be altered, resulting in a possible change in the final resolution. The results are shown in Figure 31.

A Kruskal-Wallis test was performed on the data. Test results indicate that the observed values came from three independent populations at a confidence level greater than 99.9%. Multiple comparisons made at the 95% confidence level show that all three populations are different from each other. In other words, all three coating weights gave significantly different results.

The data indicates that the highest resolution is obtained with the 2.02 $lb/10^3ft^2$ film and the lowest with the 2.52 $lb/10^3ft^2$ film.

E) Projection Exposures

Projection exposures were made with both a 6:1 649-F target and an 11:1 SO-173 target in the microcamera. The best results were obtained with the SO-173 target with a peak at 253 lp/mm. Both of these are less than the optimum reported for this film/developer system in tests performed by Perkin-Elmer. Using a prototype microcamera, developed under an Air Force contract, the Perkin-Elmer tests produced a resolution of 362 lp/mm with a 6.6:1 target.[8] A small exposure range ($<$ one stop) produced great changes in resolution ($\approx$ 30%) at each focus position.

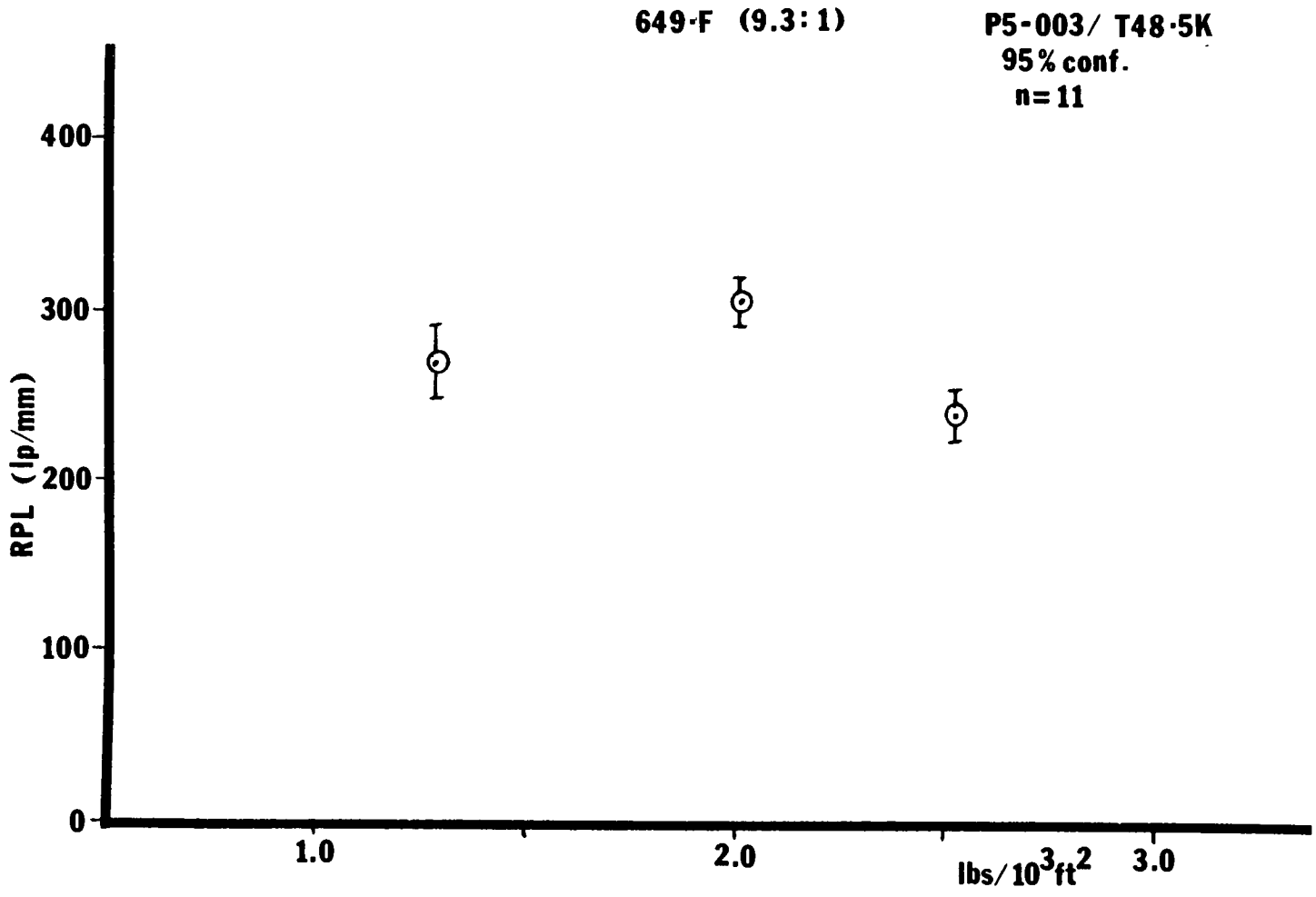

Figure 31. Resolving power limit (RPL) vs OPC coating weight in lbs/10^3ft^2. P5-003 film used with T48-5K developer.

F) SEM Observations on P5-003 Film

Contact exposures made with a 6.5:1 649-F target were viewed under an electron microscope following procedures outlined in a paper by Fritz, Hoesterey, and Brady.[53]

Photographs of the scanning electron microscope observations are presented in Appendix G. Pictures of the high frequency groups show that resolution is present in the latent image as high as 316 lp/mm. (Element six of group three is visible in the original photograph. This corresponds to 316 lp/mm.) These results confirm similar results obtained with toned images, indicating that the process is probably not developer limited.

Y-modulation scans were also done on the latent images. With a normal SEM sample, this type of scan plots a contour map related to the topography of the sample. In this case, however, the Y-modulation appears to be plotting a charge gradient contour, showing differences in charge through varying deflection of secondary electrons.

The only problem encountered was making observations under high magnification (>200X). Under these circumstances, the potential of the electron beam would charge the area in the center of the image, causing rapid deterioration of the image.

IV. Discussion

A) Silver Halide Target Comparisons

Choice of the silver halide film to use as an original target does appear to have an effect on the resulting resolution of the TEP film. In

general, a film with a higher granularity, and usually also a higher Callier Q factor, tends to produce lower resolving power on the TEP film.

In comparing the SO-173 target and the 649-F target, the latter tended to give slightly higher resolution limits even though the granularity and Callier Q factor were greater than that of the SO-173. The 95% confidence interval for the SO-173, however, was much greater than that of the 649-F, indicating a higher level of experimental error. This could account for some of the discrepancy between the results for the two films. In addition, the amount of foreign matter embedded in the SO-173 emulsion was greater than the 649-F emulsion. This particulate matter could adversely affect the contact between the target and film during exposure, thus lowering resolution. This could also explain why the experimental error was higher.

The observation of the foreign matter was made after the experimentation, so whether it occured during processing or testing can not be determined. However, since the test results trended towards lower resolutions with time, it is hypothesized that the problem was one of accumulation with time. Obviously this problem did not occur with the other targets to the same degree, so non-uniform experimental technique may have been responsible.

The Copex Pan target behaved as predicted, giving lower resolution than the 649-F or SO-173 targets. This particular film had the highest granularity and Callier Q factor, but surprisingly did not give the lowest resolution. The poorest results for all films tested were produced by the EK-3414 target.

Even though the granularity was similar to that of the 649-F film, the Callier Q factor was much higher. This may be due to the scattering effect of the matte particles on the film. The diffusing effect of this coating is apparent even by visual observation. This diffusion of the light during exposure appears to be detrimental to resolution, as indicated by the test results.

Scattering of the light rays by the silver halide grain structure is believed to be the primary cause for the optical aspect of resolution loss. A line spread equivalent to an average lateral displacement of 2.5 um should be enough to limit resolution to about 200 lp/mm. (See Appendix H.) Referring to the case shown in Figures 4 and 5, a displacement of 2.5 um for a single ray could occur from a 14 degree deflection while passing through the silver halide emulsion layer. (This case is for only a single deflection of a ray at an average emulsion depth. In reality the scattering could be much more complex, but this case is chosen as a nominal one.)

If we look at the Callier Q factor for one of the films, Copex Pan = 1.31, and convert the original density ratio to a transmittance ratio, the result shows that only 52.5% of the light passing through the silver halide film was collected by the efflux objective of the microdensitometer. This means that 47.5% of the transmitted rays fall outside a cone angle of 14.5 degrees. (The collection angle is based on the 0.25 numerical aperture for the 10X efflux objective used in the micro-densitometer.[49] The resulting lateral image displacement would then be on the order of 2.5 um, as discussed earlier. Even for the case of the SO-173 target

with a Callier Q factor of 1.10, the percentage of light outside the 14.5 degree collection angle is 24%.

In future work, separating the scattering effect from the internal reflection effect would require using a second TEP film with an ionic or semiconductive grounding layer, reducing the background density from 0.24, for the metallic type used here, to about 0.05. This would alter the reflective properties of the internal film layers. For this study, due to the large magnitude of the scattering effect, the reflection effect is considered secondary and is added into the scattering mechanism and treated as a combined optical effect.

The fact that even with a very low scattering target, such as the SO-173 or 649-F, the resolution is limited to under 400 lp/mm means that the loss in resolution is not solely due to the optical effect.

B) Charging of Silver Halide Targets

Results of pre-charging the silver halide target indicate that this procedure significantly increases the resolution of the TEP film, probably by reducing the amount of charge transfer between films during contact.

The deviation in results at each charge level, except perhaps the OV and -1073V levels, are great, probably due to the rapid decay of the silver halide surface charge. The charging procedure does not appear to cause any significant difference in resolution until the silver halide ASV approaches the ASV level of the TEP film.

Attempts were made to determine the change in ASV of the TEP film after contacting to a silver halide target. No measurable difference in ASV was observed. This does not mean that no charge transfer had occured,

only that the transfer may have been to small to be detected or may have reversed itself to its previous state when separated. The effect on resolution could result from either of these conditions.

If some portion of charge were to transfer itself to the silver halide target while contacted, resolution loss may occur due to a lateral conduction of charge carriers during exposure. (See Figure 10.) If the transfer of charge is permanent the lowering of image charge modulation remaining for development may cause a resolution loss.

Pre-charging the silver halide target appears to reduce the field in the air gap between the two films when they are in contact, preventing the transfer of charge across the separation. (See Figure 14.)

The result appears to be an increase in resolution over the non-charged samples of about 20%. These results occur only when the charge on the target is approximately equal to that on tha TEP film, indicating that minimizing the air gap field is probably responsible for the increase.

C) Water Content of Original Target

The overall result of increasing the water content of the original target was as predicted. A high water content resulted in discharging areas of the TEP film and lowering resolution. The optimum results were found at about 50% RH, the ambient condition for the testing. Below this level resolution dropped off, but not to the level of the high %RH conditions.

When the low %RH sample is removed from the preparation chamber, the film undergoes a rapid surface equilibrium with the ambient conditions before being contacted to the TEP film. It is believed that this condition adversely affects resolution, possibly through uneven adsorption or

absorption of moisture at the surface. Facilities for isolating the entire test area to a constant humidity were not available for this study, so a determination of the effect of this surface equilibration could not be tested.

In the case of the higher %RH samples, the same surface equilibration may be occuring, but the time required for the moisture throughout the emulsion to reach ambient levels is on the order of several minutes. Under the pressure of the contact vacuum, this retained moisture would be squeezed to the surface as if pressed out of a sponge. The moisture forced to the interface would act much like moisture normally present on the surface under high %RH conditions. In this way the effect of the rapid equilibration is a lesser problem.

The presence of this moisture may be responsible for conduction of charge over the image area, causing a lowering of image charge modulation.

D) Thickness of OPC Layer

The results of varying the thickness of the OPC layer were not as predicted. If the effect were solely an optical one due to the path length travelled by the exposing light, the lowest coating weight sample would be expected to give the highest resolution. The medium coating weight, however, gave the best results.

The problem in this case may be the inability to separate the optical and electrical effects during exposure. Although the electrical parameters of the three films were adjusted to obtain identical sensitometries, the manner in which the film responds electrostatically to contact with a silver halide film may also be a function of the OPC thickness.

The results of this test is valid only as an indication of the best coating weight under these conditions: 2.02 $lbs/10^3 ft^2$.

E) Projection Exposures

Projection exposure results, as compared to the Perkin-Elmer results, were poor. In fact, these results did not even meet the results obtained through contact exposure with a similar target.

Target groups as high as 600 lp/mm were visible when the projected image was viewed with the focusing scope. This modulation was not transferred to the final image on the TEP film.

Two major effects may explain this problem. First, the dependence of resolution on exposure was shown to be great. Very small changes in exposure (less than ½ stop) would greatly vary the resolution results. The power supply and the shutter mechanism could not affect a change of much less than 1/2 to 1/3 of a stop, making exposure control difficult. Secondly, the apparatus used as the basis for the microcamera, specifically the Bausch and Lomb slit illuminator, produces a high degree of flare light due to its design.[54] This flare light can cause a lowering of the image modulation, resulting in lower modulation on the TEP film.

The quality of the Perkin-Elmer/USAF micro-camera is, without doubt, better than the microcamera used for these tests. It is for this reason that contact comparisons to projected exposures will be weighted towards the Perkin-Elmer results rather than the results obtained here.

F) SEM Observations of P5-003 Film

Observations of the TEP latent images provided an indication of the potential resolution of a contact exposure before toning. Results gave

resolutions equivalent to results after toning, (316 lp/mm), proving that the results are probably not developer limited.

The useful observation time and resolution for these tests proved to be superior to previously reported results.[53]

The Y-modulation scans gave new insight into the structure of the charge gradient present in the latent image. The actual interpretation of these "topographical" plots is not understood since this scanning mode usually is used for a sample which has some depth. The depth seen in these scans is probably only due to the gradient of charge and its effect on the beam deflection.

Dark areas of the normal images and "raised" areas of the Y-modulation scans correspond to the areas discharged by the exposure; these areas have a lesser negative charge than the background.

The bright areas surrounding the bar images are unexplained, but it is hypothesized that these result from the differences in the charge at the edge. The electric field in these areas is at its strongest[55] and may be a factor in the beam deflection.

V. Conclusions

The research conducted here was initiated by a concern over the discrepancies between the contact and projection resolutions in a TEP film system. The information resulting from previous work may have provided a slightly erroreous estimate of these differences because of the choice of target used.

Much of the contact exposure work performed at James River Graphics was done using a 2:1 EK-3414 film target original.[9] Perkin-Elmer projection work was done using a 6.6:1 target.[56] The difference in the target

modulation is a factor which can cause a variation in image modulation on the TEP film. Also, the EK-3414 film was found to give the poorest resolution results due to the matte coating present on the film. These two factors give an unfair comparison for the true resolution capabilities of the film system. Unfortunately this choice of film was dictated by the contract specifications.[57]

When a high quality film target with a modulation similar to the projection target is used, the loss in resolution is much less apparent. Contact results approximate the findings of the Perkin-Elmer experiments.

The optimum resolution results, obtained with the 649-F target, were 316 lp/mm. Resolution on the silver halide target was present as high as 794 lp/mm, the maximum frequency present on the original glass Ealing target. The resulting loss in resolution when contacted to the TEP film is greater than 60%.

Using these test results, some suggestions for optimum conditions for contact exposure can be presented.

1) The target should be low in RMS granularity and Callier Q factor and be free from all foreign material, including matte coatings.

2) Moisture content of the target should not exceed the 50% RH level.

3) The silver halide target should be pre-charged to an ASV level and polarity approximately equal to that of the TEP film.

4) The optimum OPC thickness for the conditions of the tests used here is the nominal coating weight of 2 $lb/10^3 ft^2$, which is the normal weight for the P5-003 film.

Final analysis of the overall results tend to confirm the hypothesis that the cause of the resolution loss is not solely an optical or electrostatic effect, but rather can be attributed to a combination of the electrostatic characteristics of the TEP film, the electrical aspects of the physical contacting procedure, and the optical properties of the silver halide film target.

VI. Recommendations for Future Work

There are some recommendations for future work in this area: An improved measurement system could be designed for determining the amount, if any, of residual charge on the two film surfaces after contacting; further study of projection exposures and contact exposures of TEP film using various projection and illumination geometries (i.e. narrow angle vs wide angle, collimated vs diffuse) is needed; SEM observations of projection exposures could be performed; a study of positive vs. negative charging is needed; and, finally, a practical application of this study to a real world system, such as a high speed film duplication system, would be advisable.

VII References

1 P. I. Bachelder, J. F. Dirks, and G. J. Myers, "Electrophotographic Film Recording and Duplication Systems", Technical Report, Contract F-33615-78-C-1628, AFWAL/AARF, WPAFB, Ohio, 1980, pp.5.

2 R. G. Zech, J. F. Dirks, and L. M. Ralston, "Transparent Electrophotographic Films for Optical Data Storage Applications", Applied Optics, 16, 1642(1977).

3 J. F. Dirks, "Electrophotographic Film Recording and Duplication Systems", Technical Report, Contract F-33615-76-C-1312, AFWAL/AARF, WPAFB, Ohio, 1978, pp.5.

4 J. F. Dirks, "Information Recording on Transparent Electrophotographic Films", SPIE Conference, San Diego, CA, 1977.

5 R. M. Schaffert, Electrophotography, Wiley, New York, 1975, pp.557.

6 Ibid., pp.562.

7 R. P. Lubianez, and E. B. Bourgeois, "Advanced Electrodeveloper for High Performance TEP Film Applications", Technical Report, Contract F33615-80-C-1169, AFWAL.AARF, WPAFB, Ohio, 1982.

8 G. J. Myers, R. P. Lubianez, J. F. Dirks, "Continued Studies of Electrophotographic Film Recording and Duplication Systems", Technical Report, Contract F33615-80-C-1156, AFWAL.AARF, WPAFB, Ohio, 1981, pp.52.

9 Ibid., pp.54.

10 Myers, pp. 66

11 S. E. Weaver, B. W. Binns, and L. M. Ralston, "Transparent Electrophotographic Film Evaluation for High Performance Data Recording", Optical Engineering, 20, 365(1981).

12 Myers, pp.67.

13 Myers, pp.64.

14 R. J. D'Amato, "Update on Organic Electrophotographic Film Technology", IGC Conference, Andover, MA, March, 1978.

15 J. F. Dirks, "Information Recording on Transparent Electrophotographic Films", SPIE Conference, San Diego, CA, 1977.

16 R. C. Weast, Ed., CRC Handbook of Chemistry and Physics, 60th Ed., CRC Press, Boca Raton, FL, 1980, pp.c786.

17 T. H. James, The Theory of the Photographic Process, 4th Ed., Macmillan Co., New York, 1977, pp.579.

18 T. Woodlief, Jr., Ed., SPSE Handbook of Photographic Science and Engineering, Wiley, New York, 1973, pp.166.

19 Schaffert, pp.586.

20 W. J. Smith, Modern Optical Engineering, McGraw-Hill, New York, 1978, pp.167-175.

21 M. M. Shahin, "Characteristics of Corona Discharge and Their Application to Electrophotography", Photogr. Sci. & Eng., 15, 322(1971).

22 Schaffert, pp.397.

23 Schaffert, pp.556.

24 Schaffert, pp.398.

25 J. Mort and D. M. Pai, Photoconductivity and Related Phenomena, Elsevier, New York, 1976, pp.452.

26 Ibid., pp.450 - 462.

27 From Mort, pp.450.

28 G. Pfister, S. Grammatica, and J. Mort, "Trap Controlled Dispersive Hopping Transport", Phy. Rev. Letters, 37, 1360(1976); Mort, pp.vii, 450.

29 R. Lubianez, personal communication.

30 Schaffert, pp.174.

31 Schaffert, pp.456.

32 J. F. Dirks and M. B. Worwood, "Transparent Electrophotographic Process for Continuous Tone Laser Beam Recording", 32nd Annual SPSE Conference, Boston, MA, May, 1979.

33 J. Dessauer and H. Clark, Eds., Xerography and Related Processes, Focal Press, London, 1965, pp.217.

34 Mort, pp.456.

35 F. W. Schmidlin and H. M. Stark, "Lateral Conduction Mechanisms in Xerography and Their Limitations on Resolution", 22nd Annual SPSE Conference, Los Angeles, CA, May, 1969.

36 Schaffert, pp.168.

37 Dessauer, pp.405.

38 H. Kiess, Camera Sensitive Electrophotography, Focal Press, New York, 1980, pp.76.

39 W. Simm, "Studies of TESI-Processes in Electrophotography", J.A.P.E. , 4, 123(1978).

40 C. F. Gallo, "Electrostatic Aspects of Electrophotography", TAPPI Conference, Atlanta, GA, 1974, pp.115.

41 Ibid., pp.114.

42 Dessauer, pp.430.

43 Dessauer, pp.433.

44 A. D. Moore, Electrostatics and Its Applications, Wiley, New York, 1973, pp.86-89; R. G. Cunningham and H. P. Hood, U.S. 3,579,330(1971).

45 Schaffert, pp.556.

46 L. M. Ralston, personal communication.

47 R. P. Lubianez, "Transparent Electrophotographic (TEP) Process, Manual Processing Procedures", Report, James River Graphics, Inc., South Hadley, MA, 1980.

48 Isopar-G is available from Exxon Corp.

49 Woodlief, pp.838.

50 Woodlief, pp.478.

51 Ibid.,pp.976.

52 Ibid.,pp.477.

53 G. F. Fritz, D. C. Hoesterey, and L. E. Brady, "Observation of Xerographic Electrostatic Latent Images with a Scanning Electron Microscope", App. Phys. Letters, 19, 277 (1971).

54 R. Guttosch, personal communication.

55 See figure 11.

56 Ibid., pp.51.

57 Ronald Lubianez, personal communication.

58 The safelight was constructed of blue Plexiglas illuminated with a 15 watt bulb.

Appendix A Material Characteristics

Film Characteristics

Film type:	P4-005
Base:	4 mil (100 um) polyester
Conductor:	Metallic (aluminum)
Base density:	0.35
Peak sensitivity:	633 nm

Film type:	P5-003*
Base:	5 mil (125 um) polyester
Conductor:	Metallic (aluminum)
Base density:	0.40
Peak sensitivity:	595 nm

Toner Characteristics

Toner type:	T18-18
Structure:	Medium grain
Polarity:	Positive
Resolution:	Moderate

Toner type:	T48-5K
Structure:	Fine grain
Polarity:	Positive
Resolution:	High

* Coating weight variation samples have same characteristics as normal coating weight samples.

All materials supplied by James River Graphics, Inc., South Hadley, MA.

Appendix B Calculation of Average Gradient ($\bar{G}$)

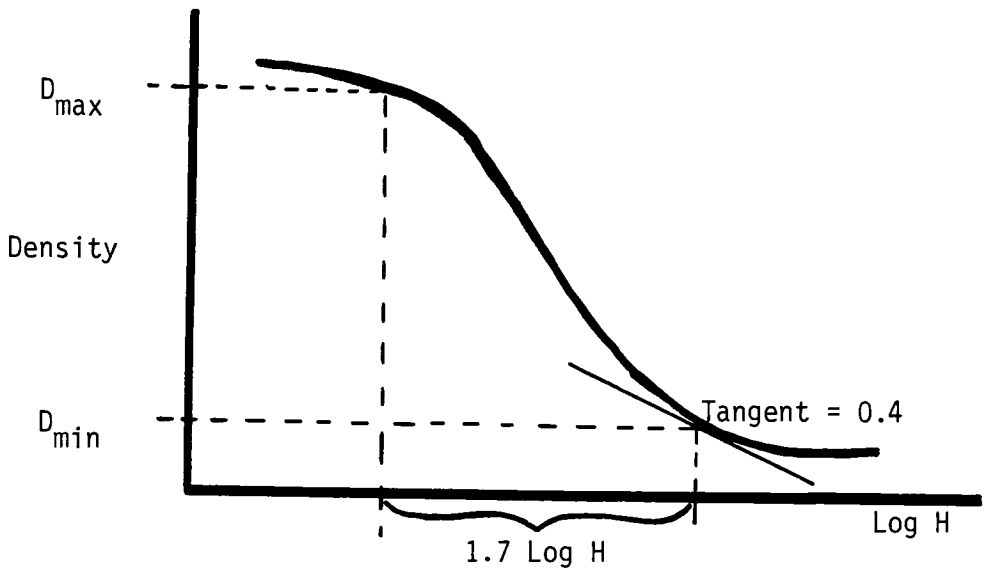

$D_{max} = D_{min} + 1.7$ Log H units

Average Gradient ($\bar{G}$) = $(D_{max} - D_{min}) / 1.7$

Speed point = $(\text{Log } H_{max} + \text{Log } H_{min}) / 2$

Figure B-1. Density vs Log H curve for positive working system.

Appendix C Manual Processing Procedures

1) Under a blue safelight[58], a small amount of the OPC layer of the film sample is removed with methyl-ethyl ketone to expose the grounding layer. The film is mounted on the vacuum platen and grounded with a small piece of conductive tape.

2) The sample is then passed under the Scorotron charging unit at a speed of 1 inch per second with a corona voltage of -6.5 kilovolts at 0.3 mA and a screen voltage of -900 volts at 1 mA.

3) The apparent surface voltage is measured by holding the vacuum plate under the electrostatic probe after charging. Output is recorded on a chart recorder.

4) The film is removed from the plate and placed in contact with the target, a vacuum is applied in the contact frame, and the sample is exposed.

5) The sample is removed from the frame and remounted on the vacuum plate. The developing tank is filled with toner and the vacuum plate and film are placed against the bias electrode. The bias voltage is initiated and the assembly is immersed into the tank. Agitation consists of lifting the assembly out of the solution for one second and repeating for ten times in a thirty second period.

6) The film is removed and allowed to drain. Two Isopar-G rinses for ten seconds each follow developing. The sample is then allowed to dry at room temperature. Room lights can be used after this point.

7) Fixing of the sample is accomplished by holding the film over a container of methylene chloride at a height of 1/4 to 1/8 inches above the liquid surface for 5 ± 0.5 seconds.

Appendix D Kruskal-Wallis Test

The Kruskal-Wallis test evaluates, by ranking, k independent samples, one from each of k possibly different populations, to test the null hypothesis that all of the populations are identical against the alternative that at lease one of the populations gives greater observed values than at least one of the other populations. The test is sensitive to differences in the means of the populations.

If the null hypothesis is rejected, the method of multiple comparisons can be used to determine pairwise which of the populations are different.

DATA: k random samples of possibly different size. The ith random sample of size n_i is denoted $X_{i1}, X_{i2},\ldots,X_{in}$. The data is arranged into i columns. N denotes the total number of observations.

A rank of 1 is assigned to the observation with the smallest value of the N observations, rank 2 to the next smallest, and so on to the largest of the N observations. In several observations have the same value, assign the average of the ranks for those observations to each. Let $R(X_{ij})$ be the rank assigned to X_{ij}, and let R_j be the sum of all the ranks of the ith column.

HYPOTHESES:

H_0: All of the k population distribution functions are identical.

H_1: The k populations do not all have identical means.

TEST STATISTIC:

$$T = \frac{1}{S^2}\left(\sum_{i=1}^{K}\frac{R_i^2}{n_i} - \frac{N(N+1)^2}{4}\right)$$

where $$S^2 = \frac{1}{N-1}\left(\sum_{\substack{\text{all}\\ \text{ranks}}} R(X_{ij})^2 - \frac{N(N+1)^2}{4}\right)$$

DECISION RULE: Reject H_0 at the α level if T exceeds the $1-\alpha$ quantile of the chi-squared distribution with k-1 degrees of freedom.

MULTIPLE COMPARISONS: The pair is considered different if the following inequality is satisfied:

$$\frac{R_i}{n_i} - \frac{R_j}{n_j} > t_1\,(\alpha/2)\,\left(S^2\,\frac{N-1-T}{N-k}\right)^{1/2}(1/n_i + 1/n_j)^{1/2}$$

where R_i and R_j are the rank sums of the two samples, $t_{1-(\alpha/2)}$ is the $1-\alpha/2$ quantile of the t distribution with N-k degrees of freedom, and S^2 and T are the equations above. The procedures are repeated for all pairs.

Appendix E ANOVA by Regression Analysis

Analysis of variance by regression is accomplished by first fitting the data to a first order linear regression equation of the form

$$Y = B_o + B_1X + \text{error} \quad .$$

$$\hat{y} = b_o + b_1x \quad Y$$

The coefficients are determined by calculation.

$$B_o \cong b_1 = \frac{\Sigma xy - \frac{(\Sigma x)\,\Sigma y)}{n}}{\Sigma x^2 - \frac{(\Sigma x)^2}{n}}$$

The ANOVA table is completed as follows:

Source	D.F.	Sum of Squares
Regression	k_1	$(\hat{y}-\bar{y})^2$
Residual	k_2	$(y-\hat{y})^2$
Total corrected	k_1+k_2	$(y-\bar{y})^2$

To test the regression for significance, the ratio of the regression SS to the residual SS/ D.F. is compared to the "t" distribution with k_1 and k_2 degrees of freedom.

Appendix F Cox and Stuart Test for Trend

The Cox and Stuart test analyzes a sequence of numbers to see if the earlier numbers are significantly different from the later numbers.

DATA: The data is arranged in order according to some criteria, in this case according to the increasing level of the independent variable %RH. The observations are then grouped into pairs (S_1, X_{1+c}), $(X_2,X_{2+c}),\ldots,(X_{n'-c},X_{n'})$, where $c=n'/2$ if n' is even, and $c=(n'+1)/2$ if n' is odd. The quantity n' represents the total number of observations and the quantity n is the number of pairs that are not tied. Each pair (X_i,X_{i+c}) is replaced with a "+" if $X_i<X_{i+c}$, or a "-" if $X_i>X_{i+c}$. Ties are eliminated.

HYPOTHESES: H_0: There is no downward trend.

H_1: There is a downward trend.

TEST STATISTIC: The test statistic T is the number of + pairs.

DECISION RULE: H_0 is rejected when T is less than or equal to t at a level of significance α, where t is from the binomial distribution with p=0.5 and n=number of non-ties. The value of y for the table entry closest to α gives t.

Appendix G SEM Observations on P5-003 Film

Photograph Identification

a) Magnification = 78X
Tilt Angle = 45°
Scan Mode = Normal

b) Magnification = 240X
Tilt Angle = 45°
Scan Mode = Normal

c) Magnification = 54X
Tilt Angle = 0°
Scan Mode = Y-Modulation

d) Magnification = 54X
Tilt Angle = 45°
Scan Mode = Y-Modulation

Photographs from ISI-40
scanning electron microscope
on following page.

Maximum resolution seen in
photograph b at 316 lp/mm.

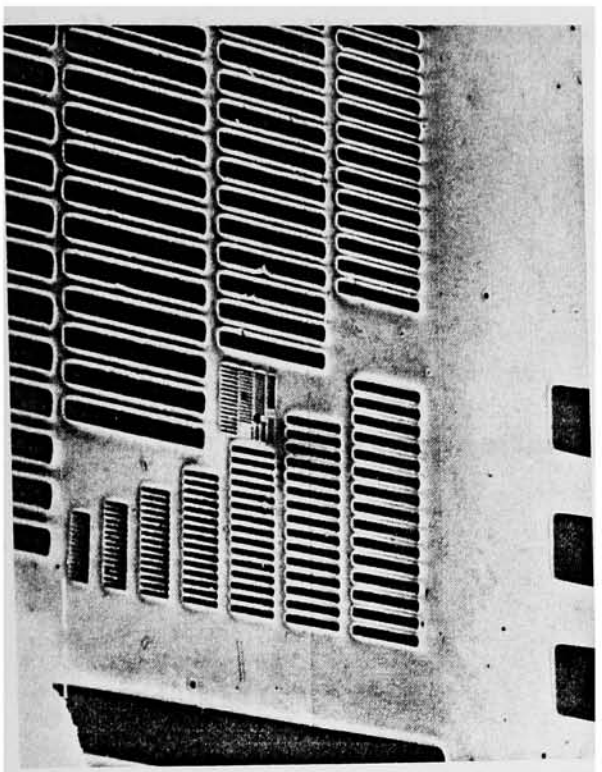

a)

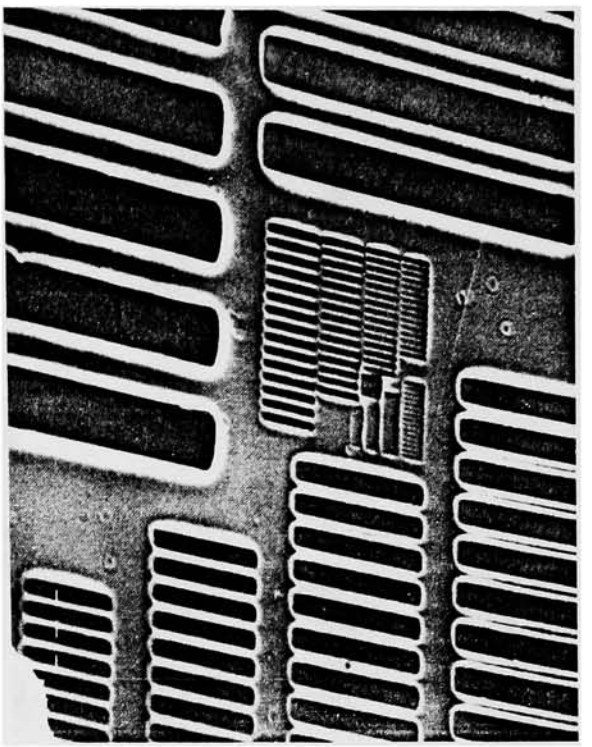

b)

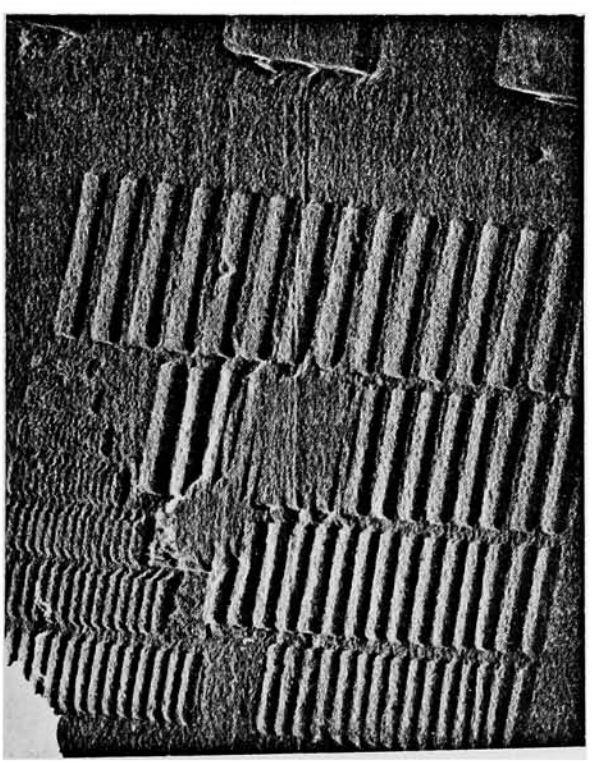

c)

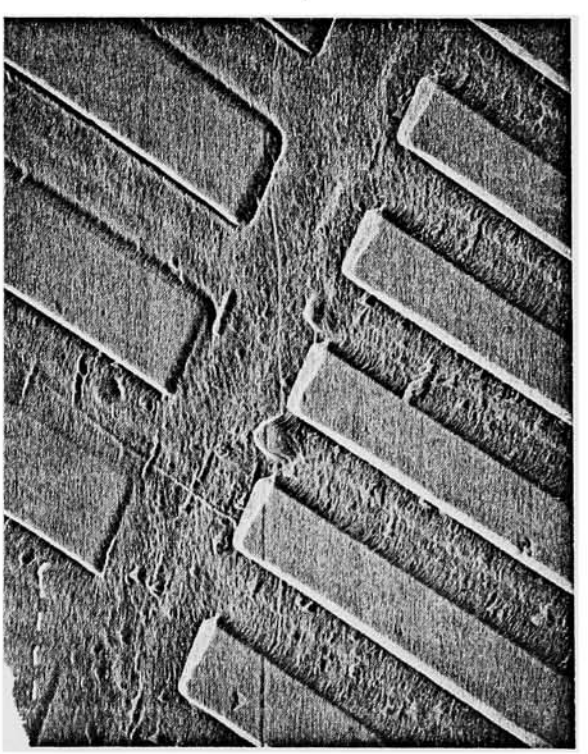

d)

Figure G-1. SEM photographs of P5-003 film.

Appendix H Tabulated Data

1) Silver halide target comparisons

	Film			
	SO-173	Copex Pan	649-F	EK-3414
Response (lp/mm)	283	251	316	200
	316	225	316	200
	316	251	316	200
	251	200	316	200
	251	225	283	200
	251	200	316	200

2) Charging of silver halide targets

	Copex Pan Target Charge Level (Volts)				
	0	-410.9	-774.2	-969.0	-1073.5
Response (lp/mm)	251	251	200	316	316
	251	200	251	316	283
	283	251	283	251	316
	251	200	251	316	316

3) Water content of original target

694-F Target

% RH	Response (lp/mm)	% RH	Response (lp/mm)
18	283	52	316
21	283	65	225
23	251	65	251
25	251	71	200
36	200	72	200
36	251	73	200
36	251	74	200
37	251	86	200
52	316	86	200
52	251	87	225
52	316	88	200
52	316		

4) Thickness of OPC layer

	649-F Target Coating Weight ($lbs/10^3 ft^2$)		
	1.32	2.02	2.52
Response (lp/mm)	316	316	200
	251	251	200
	251	316	200
	316	316	251
	316	316	251
	251	316	251
	251	316	251
	251	316	251
	251	316	251
	251	283	283
	283	316	251

Appendix I Scorotron Construction

The following pages contain mechanical drawings showing the basic construction of the Scorotron drive unit. All pieces were made from 0.064" aluminum except where noted. All dimensions are given in inches. Scales of drawings vary as noted.

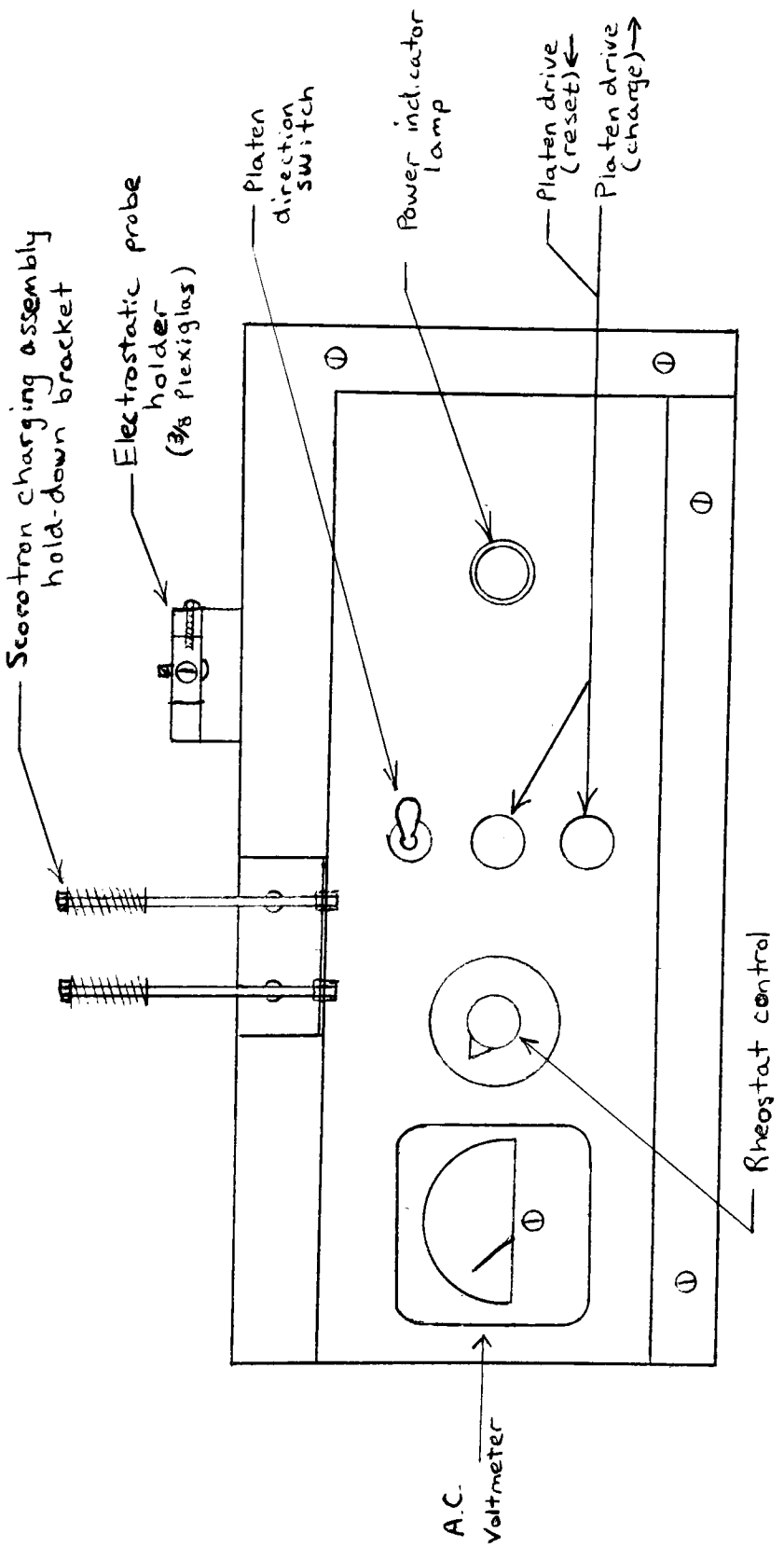

Figure I-1. Scorotron drive unit - front view of control panel. (1/2 scale)

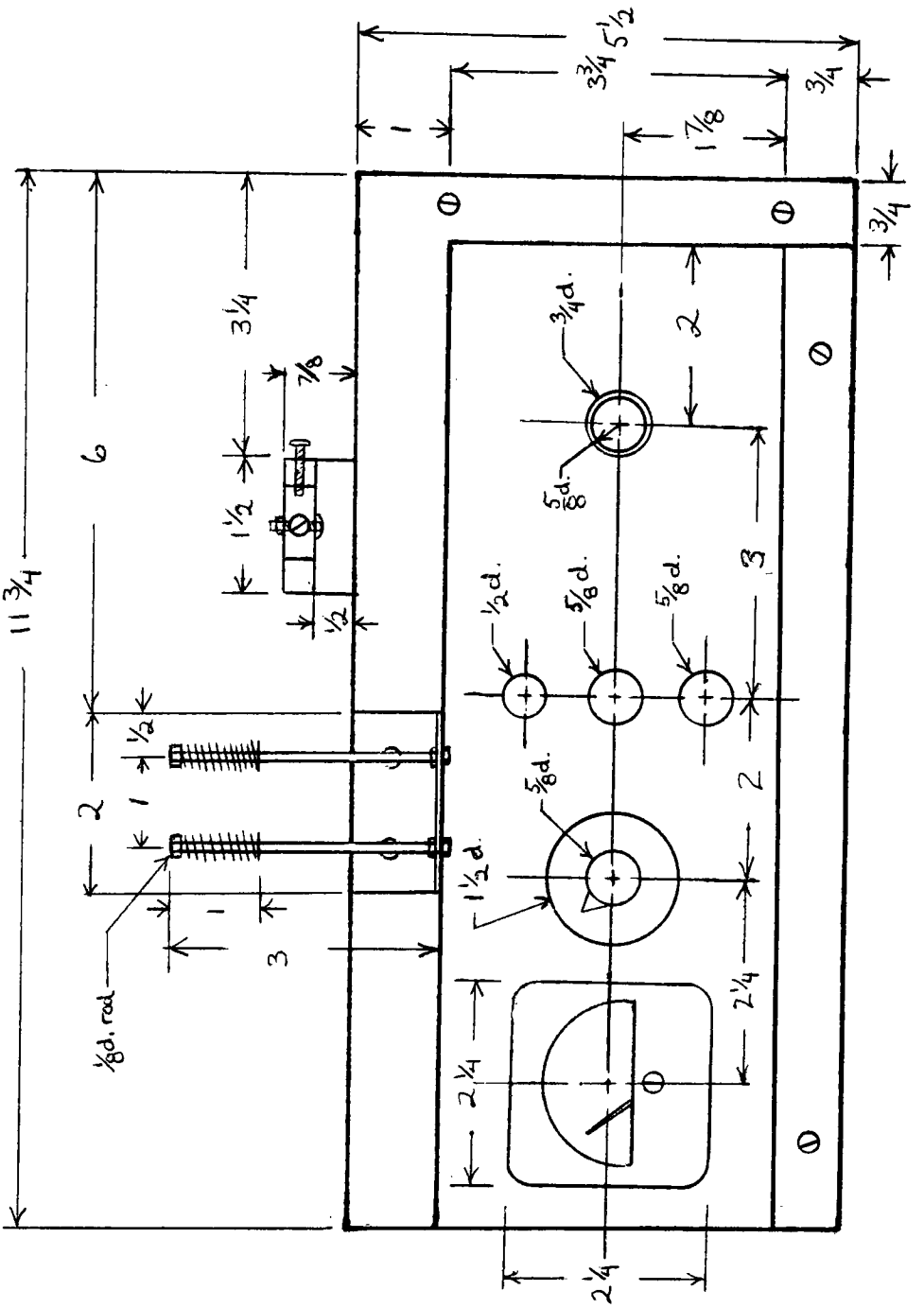

Figure I-2. Scorotron drive unit - front view. (1/2 scale)

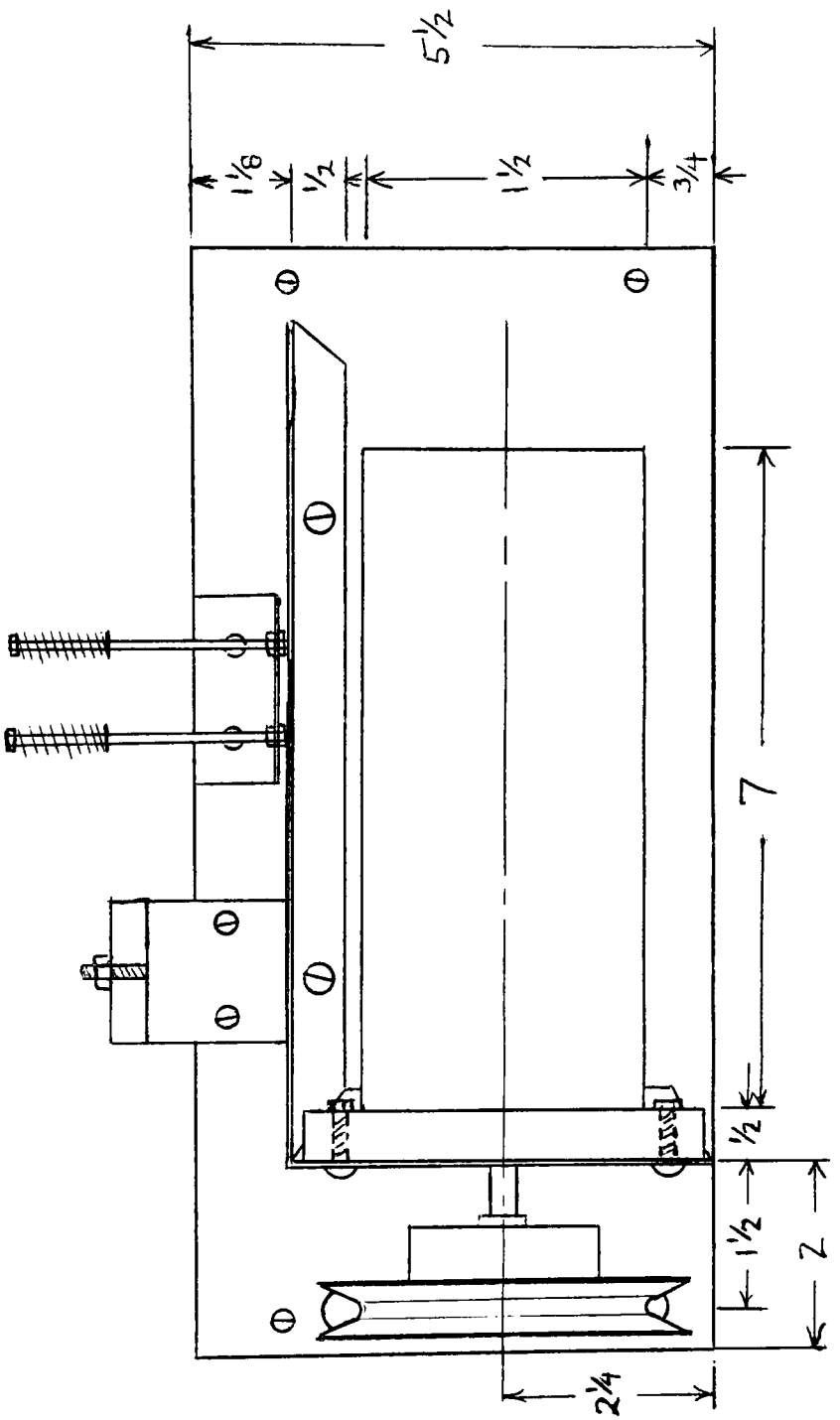

Figure I-3. Scorotron drive unit - rear view. (1/2 scale)

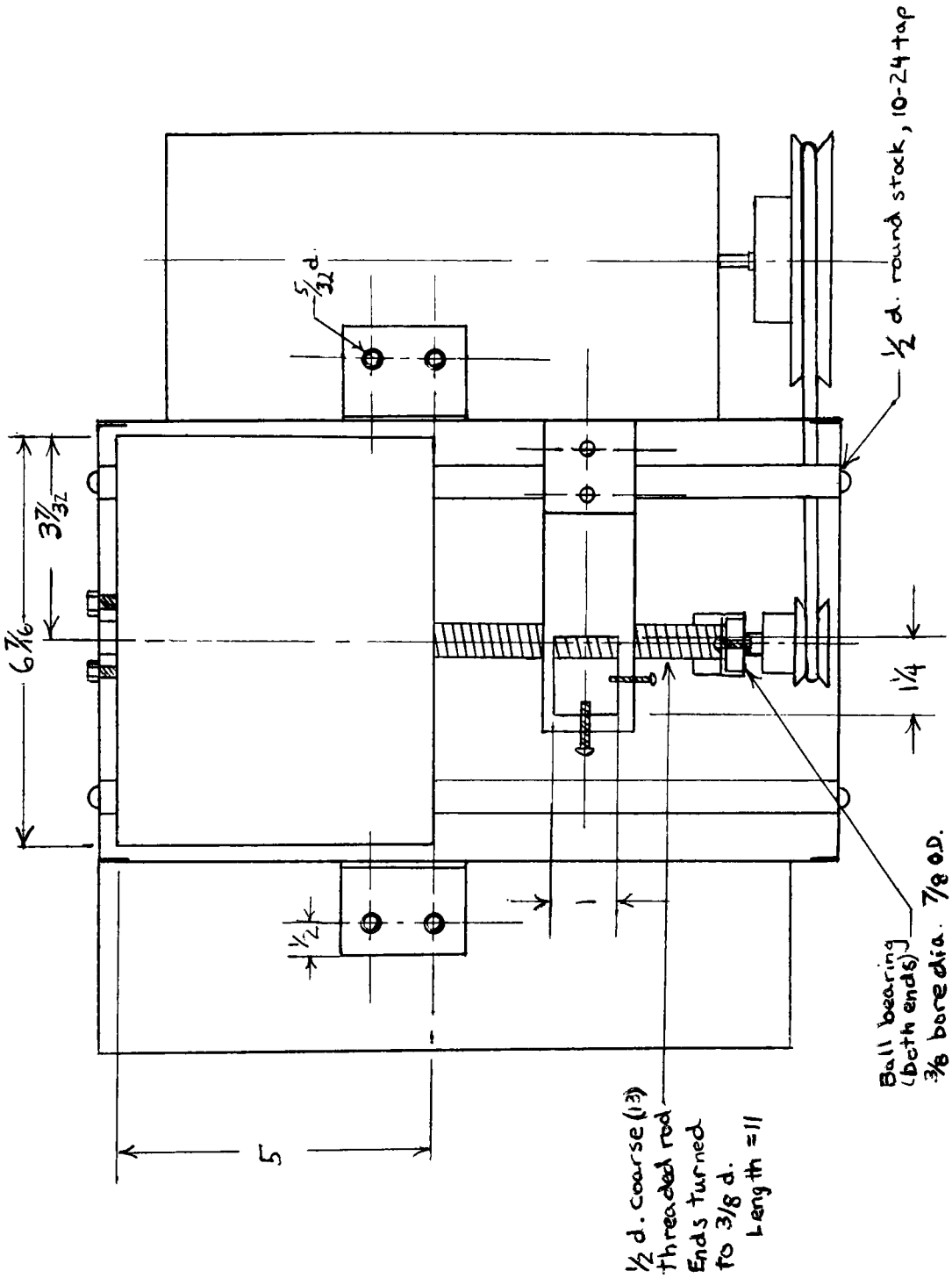

Figure I-4. Scorotron drive unit - top view. (3/8 scale)

NOTE: Drive belt = 3/16 d. x 18 circum. O-ring

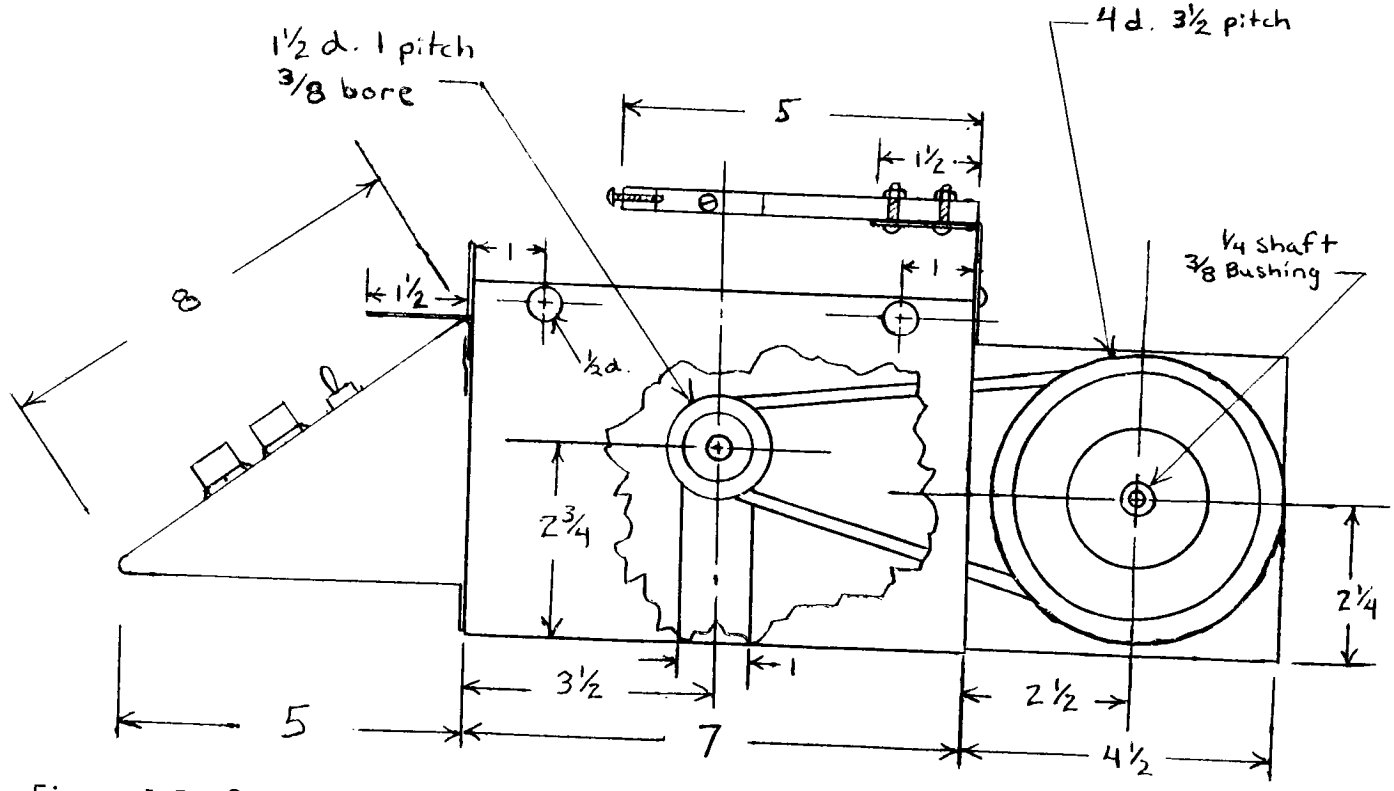

Figure I-5. Scorotron drive unit - side view. (3/8 scale)

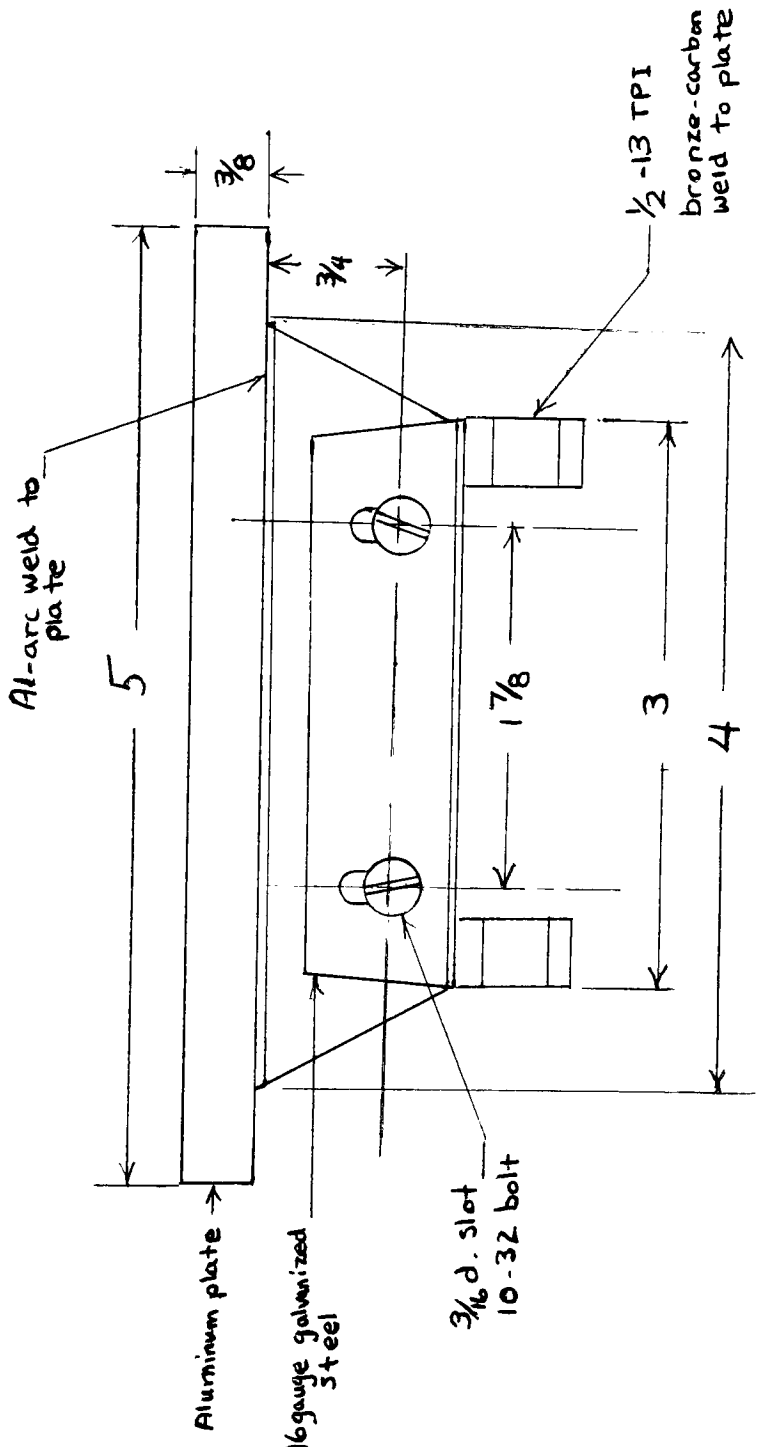

Figure I-6. Scorotron drive unit - Drive plate assembly - side view. (full scale)

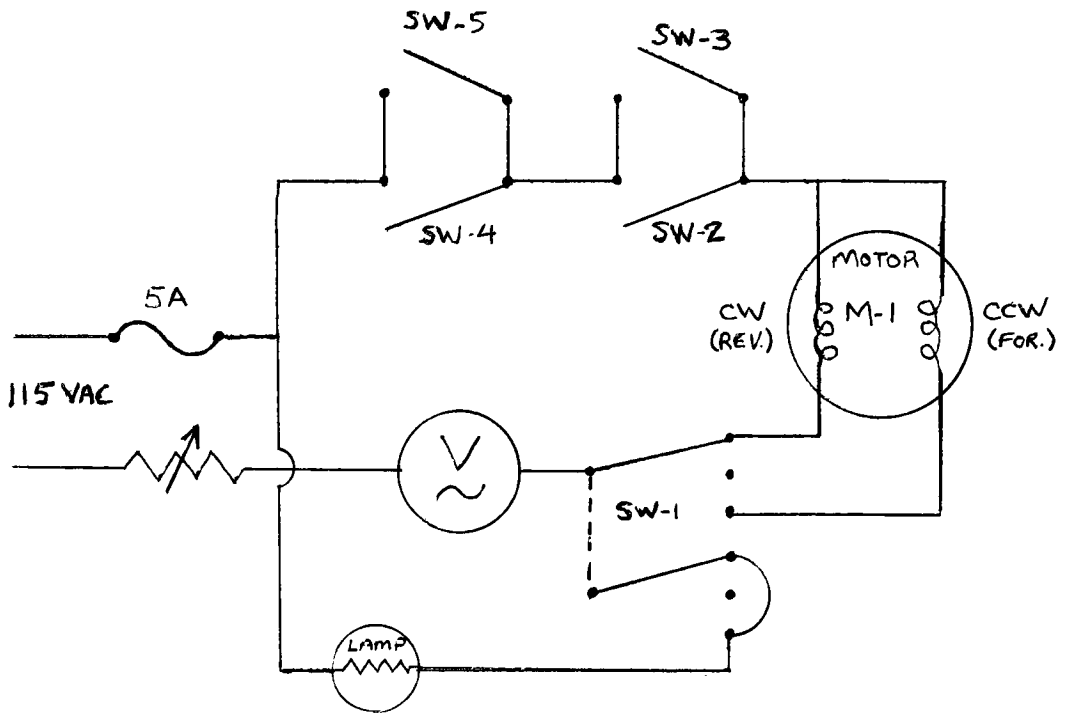

M-1 0-200 RPM DOUBLE SHADED POLE 115 VAC MOTOR
SW-1 DPDT SWITCH - DIRECTION CONTROL
SW-2 REVERSE DIRECTION LIMIT SWITCH - LEVER SWITCH (N.C.)
SW-3 FORWARD START SWITCH - MOMENTARY CONTACT (N.O.)
SW-4 FORWARD DIRECTION LIMIT SWITCH - LEVER SWITCH (N.C.)
SW-5 REVERSE START SWITCH - MOMENTARY CONTACT (N.O.)
N.O. = NORMALLY OPEN, N.C. = NORMALLY CLOSED
CW = REVERSE = RESET, CCW = FORWARD = CHARGE

Figure I-7. Electrical connections for Scorotron drive unit.

Appendix J Resolution Loss on TEP Film Resulting from Lateral Image Spread

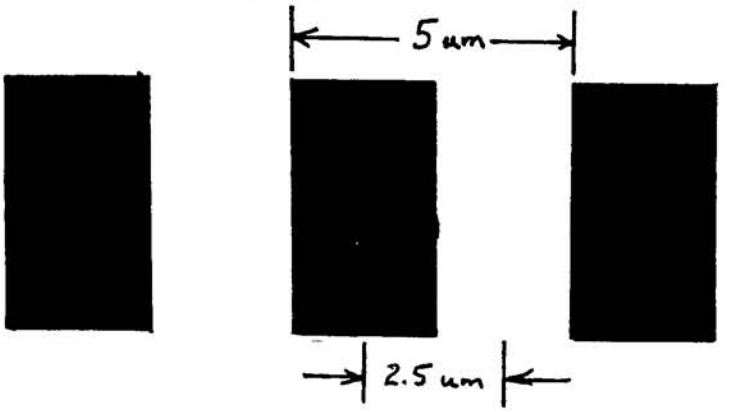

Ideal bar target shown for 200 lp/mm frequency.

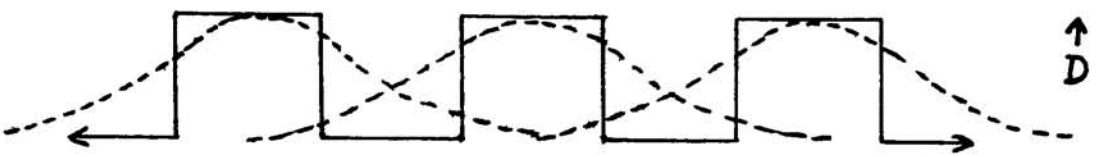

Density profile of bar target image on TEP film showing line spread due to average image point spread of approximately 2.5 um.

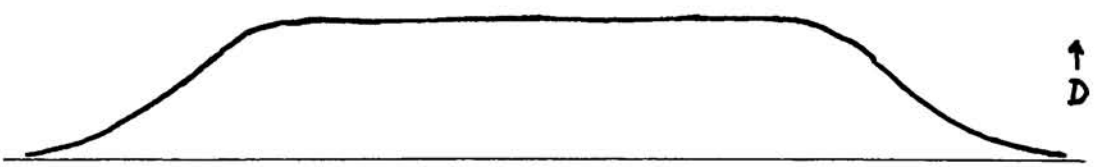

Resulting density profile after image spread. Image would be unresolved.

Figure J-1. Resolution loss on TEP film resulting from lateral image spread.

VIII Vita

Thomas Charles Sutter was born on August 30, 1960 in Holyoke, Massachusetts. He attended high school in West Springfield, Massachusetts where his parents currently reside. Mr. Sutter enrolled in the Photographic Science and Instrumentation program at the Rochester Institute of Technology in September of 1978. In September of 1981, Mr. Sutter enrolled in the Master's degree curriculum of the same program.

From June of 1981 to August of 1983, Mr. Sutter worked as a Graduate Teaching Assistant for the Photographic Science and Instrumentation Division while continuing his studies. During 1983 the curriculum name was changed to the Imaging and Photographic Science program.

In September of 1983, Mr. Sutter was employed full-time by AT&T Technologies, Inc., (formerly Western Electric, Co., Inc.), in Richmond, Virginia. His work as a Process and Development Engineer includes aqueous liquid polymers, high collimation printers, automated handling equipment, and photo-tool generation methods.

Mr. Sutter was married in October of 1983 and currently resides in Richmond, Virginia.